Carbon Dioxide Capture by Adsorption on a Biomass Based Activated Carbon

by

SAHAND SAEIDI HARZAND

Submitted to the Graduate School of Engineering and Natural Sciences
in partial fulfillment of the requirements for the degree of
Master of Science

Sabancı University

June 2018

TITLE OF THE THESIS/DISSERTATION

APPROVED BY:

Asst. Prof. Dr. Alp Yürüm (Thesis Supervisor) .....

Prof. Dr. Yuda Yürüm (Thesis Co-advisor) .....

Prof. Dr. Emin Arca .....

Prof. Dr. Serhat Yeşilyurt .....

Assoc. Prof. Dr. Burç Mısırlıoğlu .....

Carbon Dioxide Capture by Adsorption on a Biomass Based Activated Carbon

Sahand Saeidi Harzand
Materials Science and Engineering, M.Sc. Thesis, 2018
Thesis Advisor: Asst. Prof. Dr. Alp Yürüm
Thesis Co-Advisor: Prof. Dr. Yuda Yürüm

ABSTRACT

Adsorption of carbon dioxide has been examined on activated carbons produced from sunflower's stem pith. Interesting structure and abundance of this agricultural residue make it a good candidate for the AC's precursor role. The AC samples are produced with a combination of physical and chemical activation methods. Two alkali hydroxides of KOH and NaOH are selected as the activation agents. FTIR, TGA and BET tests are done on the bio-chars and activated carbon produced to study the structure of them. Higher temperatures and longer carbonization, cause the elimination of more functional groups from the raw material and a bring a higher surface area to the synthesized bio-chars and ACs. The highest surface area for NaOH and KOH activated samples are measured as 2948.43 and 2267.52 m^2/g, respectively. In this study, NaOH, as the activation agent, provides higher surface area but KOH produces higher micropore to total volume ratio of 0.78 and 2.08 nm average pore diameter. This pore size distribution is more favorable for carbon dioxide adsorption than of NaOH which are measured as 0.68 micropore to total volume ratio and average pore diameter of 2.63 nm. Therefore, in the adsorption pressure range of 0 to 8 bars, KOH activated samples demonstrate higher adsorption capacity than AC activated by NaOH. For NaOH activated samples, shorter carbonization time does not cause any significant difference in the CO_2 uptake. In case of KOH, in the pressure range of 0 to 2 bars, the uptake difference is negligible, but for higher pressures, carbon dioxide adsorption capacity increases by increasing the carbonization time. Moreover, thermodynamic analysis about the isosteric heat of adsorption and Gibbs free energy of the samples activated by KOH, indicates that the CO_2 adsorption on AC is exothermic and a physisorption process.

Biyokütle Tabanlı Aktif Karbon Üzerinde Adsorpsiyon ile Karbon Dioksit Yakalama

Sahand Saeidi Harzand
Malzeme Bilimi ve Mühendislik, Yüksek Lisans Tezi, 2018
Tez Danışmanı: Dr. Öğretim Üyesi Alp Yürüm
İkincil Tez Danışmanı: Prof. Dr. Yuda Yürüm

ÖZET

Karbondioksitin adsorpsiyonu, ayçiçeği sapından elde edilen aktif karbonlar üzerinde incelenmiştir. Bu tarımsal atığın ilginç yapısı ve bolluğu, bu malzemeyi aktif karbon (AC) hammadesi olarak kullanılması için iyi bir aday yapmaktadır. AC örnekleri, fiziksel ve kimyasal aktivasyon yöntemlerinin bir kombinasyonuyla üretilmiştir. Alkali hidroksit olarak KOH ve NaOH aktivasyon ajanı olarak seçilmiştir. FTIR, TGA, BET analizleri, üretilmiş biyo-kömür ve aktif karbon örneklerinin yapılarını incelemek için yapılmıştır. Yüksek sıcaklıklar ve daha uzun karbonizasyon, fonksiyonel grupların hammaddeden daha fazla uzaklaşmasına ve sentezlenmiş biyo-kömür ve AC'de daha yüksek yüzey alanı elde edilmesine sebep olmuştur. NaOH ve KOH aktif örnekleri için en yüksek yüzey alanı sırasıyla 2948.43 ve 2267.52 m^2/g olarak ölçülmüştür. Bu çalışmada aktivasyon ajanı olarak NaOH ile daha yüksek yüzey alanı elde ederken, KOH ile 0.78 gibi daha yüksek mikrogözenek/toplam gözenek hacmi ve 2.08 nm gibi daha küçük ortalama gözenek çapı elde edilmiştir. Bu çeşit gözenek dağılımları karbon dioksit adsorpsiyonu açısından NaOH ile elde edilen değerlere göre daha uygundur. NaOH ile mikrogözenek/toplam hacim oranı 0.68 ve ortalama gözenek çapı 2.63 nm olarak ölçülmüştür. Bu sebeple 0 ile 8 bar basınç aralığında, KOH aktifleştirilmiş numuneler ile, NaOH ile aktive edilen AC'lere göre, daha yüksek adsopsiyon kapasitesi elde edilmiştir. NaOH ile aktivite edilmiş örneklerde daha kısa karbonizasyon süresi karbondioksit adsorpsiyonunda belirgin bir fark yaratmamıştır. KOH ile aktivasyonda ise 0 ile 2 bar basınç aralığında ciddi bir fark elde edilmezken, daha yüksek basınçlarda karbonizasyon süresiyle adsorpsiyon miktarı artmıştır. Ayrıca KOH ile aktivite edilen örneklerde yapılan izoterik adsorpsiyon enerjisi ve Gibbs serbest enerjsi termodinamik analizleri, KOH ile aktive edilmiş AC üzerinde CO_2 adsorpsiyonunun ekzotermik ve fiziksel tutunma olduğunu göstermiştir.

AKNOWLEDGMENTS

Foremost, I would like to express my sincere gratitude to my advisors Prof. Dr. Yuda Yürüm and Assist. Prof. Dr. Alp Yürüm for the continuous support of my master's study and research, for their patience, motivation, enthusiasm, and immense knowledge. Their guidance helped me in all the time of research and writing of this thesis. I could not have imagined having a better advisors and mentors for my study.

Besides my advisor, I would like to thank the rest of my thesis's jury members, Prof. Dr. Emin Arca, Prof. Dr. Serhat Yeşilyurt and Assoc. Prof. Dr. Burç Mısırlıoğlu, for their encouragement, insightful comments.

My sincere thanks also goes to my fellow lab mates in Sabancı University, Dr. Zahra Gohari Bajestani, Dr. Mustafa Baysal and Aysu Yurduşen for their helps and supports. Without their knowledge and guidance this study was hardly possible. Likewise, I thank the family of Materials Science and Engineering program at Sabancı University. I also should express my gratitude to Sabancı Unıversity gor its support and providing such an environment for advancement and growth in science and technology.

Last but not the least, I would like to thank my beloved friends for supporting me spiritually and standing beside me.

To those who brought me into this world
and gave me my name

and
to my little sister
who was a material scientist before me

CONTENTS

FIGURES

TABLES

CHAPTER 1

1. INTRODUCTION

Development of the modern societies has led to higher and higher fossil fuel consumption. As one of the negative side effects of utilization of fossil fuels, the carbon dioxide emission rate has been drastically increasing over the past years. Energy, transportation and industries, which are vital aspects of a modern civilization, are the main sources of CO_2 emission into the atmosphere [1]. According to Mauna Loa Observatory, the concentration of CO_2 in the atmosphere has passed the symbolic 400 ppm threshold mark, permanently and will not return below that value for lifetimes [2].

Effects of the carbon dioxide emission do not need any further discussion for everyone is familiar with these destructive phenomena's such as global warming, climate changing, increasing sea levels and endangering the existence of different species. Hence, the need for reduction of the concentration of greenhouse gases, mostly carbon dioxide, is eminent more than ever. International agreements such as 1977 Tokyo protocol of the United Nations Framework Convention on Climate Change (UNFCCC) or 2015 Paris agreement reached at the conference of parties (COP21) by the Intergovernmental Panel on Climate Change (IPCC), indicates the global concern about this matter.

Capturing CO_2 from its main emission sources, such as fossil fuel power plants or industrial facilities such as cement plants, and its sequestration which is also known as Carbon Capture and Storage (CCS) is considered as one of the major solutions to address the environmental problems of global warming and climate change [3].

There are three methods introduced as primary approaches to carbon dioxide capture from different fuel combustion processes: pre-combustion; post-combustion; and oxyfuel. Among these methods, the post-combustion process is the most practical one for convenient installation on existing plants, being applicable on all hydrocarbon based energy generations, and its economic advantages compared to other methods. The post-combustion process itself can be divided into many sub-categories such as absorption, adsorption, cryogenic, membrane technologies, etc.

The absorption processes for taking away CO_2 from a gas stream have been applied on an industrial scale for more than 50 years. It is based on the exothermic reaction of a sorbent with the CO_2 content of an exhaust gas stream, preferably at low temperatures. The reaction is then reversed in a regeneration process at rather higher temperatures. Despite of the highest carbon uptake of absorption process among the other

processes, it has some drawbacks. Its low energy efficiency, due to high temperature requirement for the regeneration, higher installation and running costs and not being able to have an efficient performance in high pressures are some of the reasons to develop an alternative method for absorption.

In contrast to absorption, in which the absorbed molecules make a solution along with the solvent, adsorbed molecules remain on the surface of the sorbent. Adsorptive gas separation has been industrially used as long as absorption-based technologies, having been initially driven primarily by air purification applications. Adsorption processes use solid sorbents and have many advantages over the absorption into liquid sorbents. No need for high temperature and ergo better energy efficiency, minimum pressure drop, low cost for sorbent synthesis, environmentally benign and easily disposable solid waste, and a wide range of operating temperatures are some of these merits. Hence, adsorption can be considered as the most promising and adaptable method between other available processes likes absorption, cryogenic separation and membrane separation.

Among many options for the role of the sorbent, activated carbons (ACs) are found the most suitable for adsorption of carbon dioxide compared to others. They exhibit high adsorption capacity, fast kinetics, high surface area, better pore size distribution and thermal stability [4]. They are also inexpensive and insensitive to moisture. Adsorption of gases or vapors onto activated carbons is widely utilized in different applications like separation and purification of gases, gas storage systems, adsorption-based heating and cooling systems and energy storage systems [5].

In this study, a thorough investigation has been derived for the carbon dioxide adsorption performance of activated carbons from sunflower's stem. One of the challenges in the commercial manufacturing any sorbent, independent of the capturing process, is to introduce cheap precursor. Here, the raw material for synthesizing AC is from an agricultural waste, eliminating the initial cost of the resource purchasing. Moreover, this biomass source has shown a rather high porosity among other available options; Which helps to develop a sorbent with a higher surface area and better adsorption uptake.

1.1. Carbon capturing

Started by the industrial revolution in the 17th century and following that with the technological revolution, human activity and style of living caused a breakdown in carbon dioxide emission. By burning all that fossil fuel i.e. coal, oil and natural gas, all the CO_2 from the early ages of the planet Earth, 360 million years ago, which was trapped in deep layers beneath the surface, started to get released into the atmosphere. Three major sources of CO_2 emission are power generation, transportation and industries. Power generation alone is responsible for about a third of net carbon emission into the atmosphere [1, 6].

Carbon capture, or as its complete name Carbon Capture and Storage (CCS), refers to technologies and methods that collect carbon in the form of carbon dioxide (CO_2) at some stage of the processes such as combustion or gasification [7]. The Collaboration of multiple fields of science and engineering is essential for this purpose. Understanding the physical and chemical characteristics of the different CO_2 emissions sources serves as a critical first step. Process engineering, materials science, catalysis and nanoscience will play key roles in merging the various technologies toward an integrative approach to meet the challenge.

For each emitter sections there are many capturing methods introduced. For example, in power generation based on how the fuel is utilized in the cycle, three approaches are defined; post-combustion, pre-combustion and oxy-fuel [8]. But apart from which method or mechanical perspective for the carbon capturing is used, all methods share one common and vital step, separating CO_2 from a gas mixture stream. Existing processes of CO_2 removal from a gas stream are based on physical or chemical separation and divided into absorption, adsorption and cryogenic processes [9]. All these techniques have their own merits and demerits which should be taken into account to choose the best and the most effective option.

1.1.1. Absorption

Absorption is a process that relies on a solvent's chemical attraction with a solute to preferably dissolve one species over another. In carbon capturing by absorption a solvent dissolves CO_2, but not any other components of a gas flue stream such as oxygen or nitrogen. The carbon dioxide fused solution is pumped through a regeneration column, where the CO_2 is separated from it and stored. The recycled solvent is used again in the

cycle for a new batch of flue gas. The drawback of this process is a considerable heat required for the regeneration step. In this step the CO_2-rich solution is heated for carbon to be stripped. This heat is provided by fuel combustion which causes excess CO_2 release and efficiency drop [6, 7]. Figure 1 illustrates the schematics of a chemical absorption system.

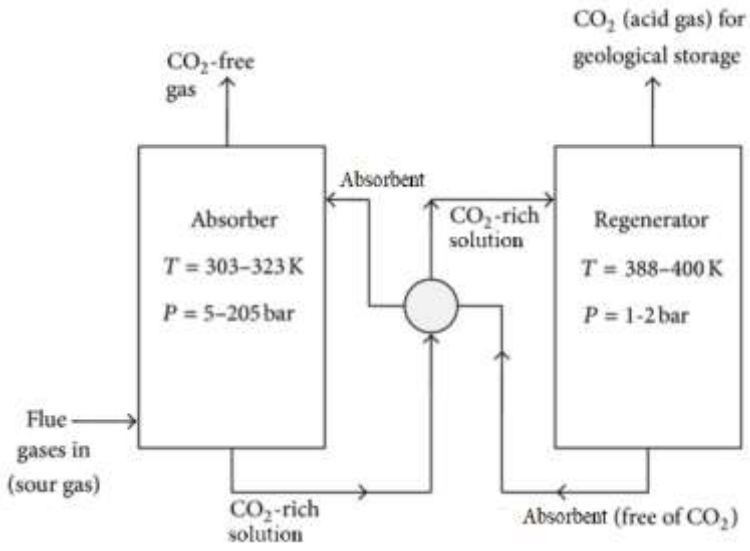

Figure 1. Chemical absorption system's schematics

While absorption method has some advantages, it is highly energy consuming which results in a high-cost. Emission of carbon dioxide from power plants can significantly be reduced by absorption. However, the separation process consumes 25 to 40% of the plant's energy and costs about 70% additional fees [10]. Additionally, the sulfur based components of the gas stream (SO_x gases) degrade the solvents used in the process. It has been reported that approximately 1.6 kg of solvent is lost for each ton of captured carbon dioxide [6]. These and many other problems bring the focus to other methods of CCS.

1.1.2. Cryogenic separation

Unlike absorption, cryogenic CO_2 separation is a completely physical process. Gas separation by cryogenic distillation relies on differing boiling points of the components in a flue gas stream. Cryogenic distillation is done by cooling the stream to

carbon dioxide's boiling point and collect it afterward. Under the right pressure and temperature, the triple point of CO_2 at -56.6 °C and 7.4 atm, carbon dioxide will condense while nitrogen stays in its gaseous form [6]. This allows N_2 to exit the system and CO_2 be captured easily.

In cryogenic separation CO_2 will be in liquid phase at the end which is the advantage of this process over the others. But the energy required for achieving to this low temperature makes it ineffective. Moreover, all NO_x, SO_x, O_2 and H_2O component of the stream should be removed before the CO_2 capturing step. If water enters the chambers it will freeze inside and shut down the whole system.

1.1.3. Adsorption

Considering all disadvantages of previous methods, which cannot be ignored, adsorption can be considered as the most promising carbon capturing methods among others likes absorption, cryogenic separation and membrane systems. The advantages of adsorption over other techniques are cost reduction of CO_2 separation, carbon capacity increases, lower regeneration energy requirements, reducing pressure drop [5], no regeneration, ease of adding to power or industrial plants, and absence of phase change which leads to increasing the efficiency [8]. Also unlike absorption and cryogenic separation where the vessels should withstand corrosive solutions or severe low temperatures, here they only have to tolerate small pressure or temperature changes.

Contrasting absorption in which CO_2 was solved into a liquid solvent, in adsorption process, due to interactivity between molecules, CO_2 particles are trapped inside a solid porous sorbent [6]. In adsorption molecules of carbon dioxide can be attached loosely by weak intermolecular forces, as it is called physisorption, or strongly by covalent bonding, also known as chemisorption. Generally, as a rule of thumb, physisorption occurs for the heat of adsorption of 10 to 15 kcal/mol or less, while chemisorption occurs for higher values [8].

In this process, a component prior to adsorption in its fluid status is referred as the adsorptive and once trapped it is defined as the adsorbate. The catching solid surface is known as the adsorbent, or in more general term sorbent, in case of having both adsorption and desorption processes together.

1.1.1.1. Chemical adsorption

In case of chemical adsorption or chemisorption, strong covalent bonds form on the surface between adsorbent and adsorbate's molecules. Basic organic groups (amine) and inorganic metal oxides (alkali metals or alkali-earth metals) are the most popular high surface area subjects for this reaction.

Amine-based adsorbents are widely studied due to their lower heat of regeneration rather than aqueous amine solutions used in the absorption process. But their low carbon dioxide capacity and high costs are some major drawbacks for commercialization and industrial scale application [11].

1.1.1.2. Physical adsorption

Physical adsorption or physisorption is mainly linked with van der Waals forces, or dispersion-repulsion forces. The relationship between the adsorbed amount of the adsorbate on the surface of adsorbent is expressed by a set of graphs known as adsorption isotherms.

Although, the shape of isotherms is dependent on many factors i.e. interaction of components of the stream to each other in the confined pore space, the interaction of components with the pore wall, and also in the case of micropore the wall-wall interaction of pore [8]. The International Union of Pure and Applied Chemistry (IUPAC) has classified pores according to their size.

Table 1. Pore size classification

Type	Pore Size (nm)
Micropore	< 2
Mesopore	2 – 50
Macropore	> 50

In 1985, IUPAC divided the adsorption isotherms in a six-groups classification. During past years some differences and updates have been added to the isotherms but the basics remain unchanged. This classification is shown is shown Figure 2 [12].

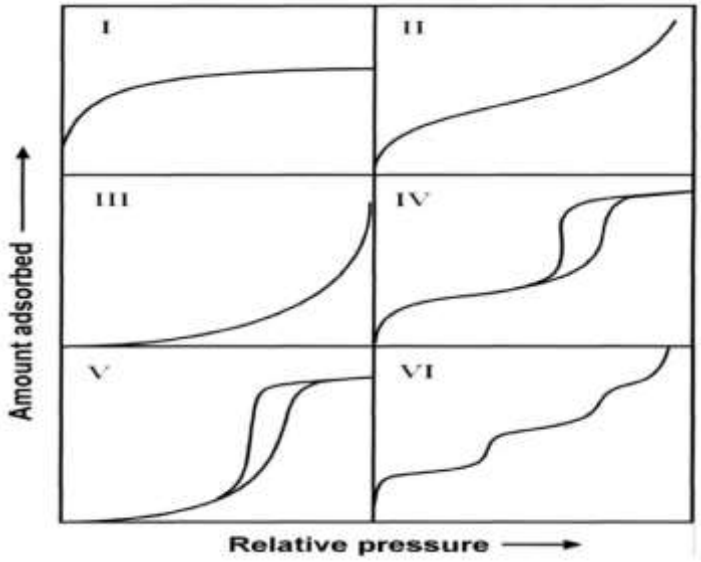

Figure 2. Classification of physisorption isotherms

Type I isotherms happen by monolayer microporous solids having relatively small external surface area, e.g. molecular sieve zeolites or activated carbon. This kind of isotherms is concaved to the relative pressure and seems to have a limiting value for the adsorbent uptake. This limiting uptake is mainly determined by the micropore volume rather than the whole surface area. As it is seen from the Figure 2, there is a steep growth in amount adsorbed at low relative pressures ($^{P}/_{P_0}$) which is due to the interaction of adsorbent and adsorbate in narrow micropores (molecular size micropores) resulting in micropore filling in very low pressures. Type I isotherms are given by materials having mainly narrow micropores (< 1 nm) or with a broader distribution range of micropores and maybe narrow mesopores (< 2.5 nm).

Type II isotherms occur by the adsorption on nonporous and macroporous materials. The shape of the graphs is resulted by unrestricted monolayer-multilayer adsorption up to high values of relative pressure. The knee in the isotherm indicates the completion of the monolayer coverage. The absence of any identifiable monolayer formation on the adsorbent gives the type III isotherms, the interaction of components are relatively low and adsorbed particles are clustered on the surface of nonporous or macroporous materials.

Type IV isotherms represent adsorption on mesoporous materials which is determined by the interaction of adsorbent and adsorbate and also the interaction of

molecules in the condensed state. The initial monolayer-multilayer adsorption on the mesopore walls is followed by the pore condensation. This type of isotherms is accompanied by a hysteresis which happens when the pore width surpasses a critical value. Type V isotherms are basically the Type III adsorptions accompanied by a hysteresis.

In the case of type VI isotherms, a layer by layer adsorption on a highly uniform nonporous surface is going on. Each knee on the graph stands for a layer's filling completion [13].

1.1.1.3. CO_2 adsorption

For carbon dioxide adsorption both chemisorption and physisorption can happen. However, due to the high volume of gas to be handled, in order to minimize the required energy for regeneration, it is probable that physical adsorption will be considered as the primary technique, in term of material and set-up design, for this application. Also, it should be mentioned that carbon dioxide adsorption has a spontaneous and exothermic nature [5, 8].

It is reported that the carbon dioxide adsorption is based on the type I isotherms and can be described by Langmuir adsorption equation, or Langmuir isotherms [14]. The isotherms generally represent the relation between the amount of adsorbed component per unit of adsorbent versus the pressure change. Langmuir equation can be expressed as:

$$\theta_{eq} = \frac{KP}{1 + KP}$$

where θ_{eq} and P are equilibrium surface coverage and pressure, respectively. K, the adsorption-desorption ratio, is defined as below:

$$K = \frac{\alpha e^{Q/RT}}{\beta (2\pi mkT)^{1/2}}$$

in which, α and β are adsorption and desorption constants, Q is the heat of adsorption, T is the absolute temperature, m is the adsorbate particle's mass, and R and k are gas and Boltzmann constants, in that order.

Pressure swing adsorption (PSA) and temperature swing adsorption (TSA) are two of the main methods for carbon capture and storage via physical adsorption. In either

case, the rate of carbon uptake depends on the partial pressure, temperature, pore size of the sorbent and interaction forces between CO_2 and adsorbent [6]. Because of the lower energy requirement, the simplicity of the facilities and higher rate of regeneration, PSA is considered superior to TSA.

Figure 3 shows a typical PSA system. At this configuration, after cooling the gas stream, preferably at about 30 °C, flue gases enter a chamber where the adsorbent is located in. The chamber is pressurized by the flue gases with a compressor to maximize the CO_2 adsorption. Meanwhile, other components of the flue stream are allowed to leave the chamber, meanwhile. Then desorption process begins by applying a vacuum to the chamber. CO_2 molecules leave the surface of the adsorbent. The gaseous carbon dioxide can be collected separately and stored for the further steps. Currently, to maximize the efficiency of the systems, two chambers work side by side each other, as the double chamber adsorption systems. In this case, while CO_2 is adsorbed in one of the chambers, the other one is in desorption stage. This configuration increases the rate of the procedure and guarantees the continuity of stream flow.

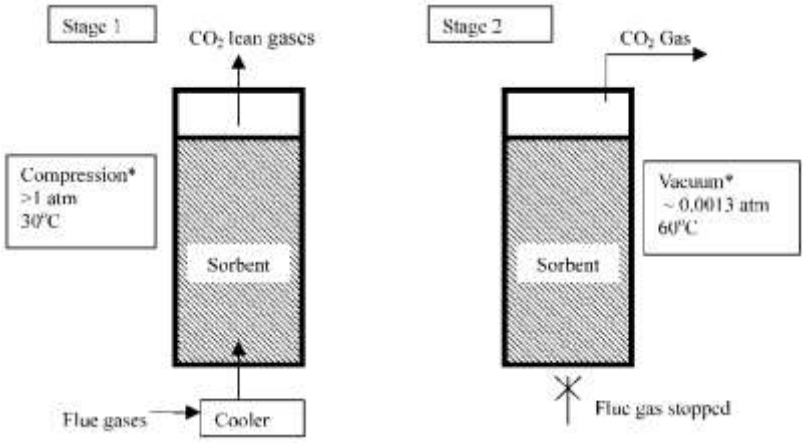

Figure 3. Pressure swing adsorption (PSA) system

1.2. Adsorbents

Selecting a perfect sorbent is a complex process. Adsorbent materials should satisfy some critical criteria to provide an efficient system, both economic and

operational, to capture and store carbon dioxide from the flue gas stream. These criteria are as follows [3]:

1) Adsorption capacity: The adsorption capacity of a sorbent is represented by its adsorption isotherms, as explained before. This value is of paramount importance to the economic aspects of the capturing system because it determines the required amount for the system, which also determines the size of vessels [15].
2) Selectivity: Ratio of carbon dioxide capacity of a sorbent to that of another component at a stream has a direct impact on the purity of CO_2 adsorbed and system's size, as well. The purity of CO_2 is an important aspect of sequestration. Flue gas stream from a power plant which burns fossil fuel as the energy source, contains a high amount of nitrogen, oxygen and water vapor. It is important for a good sorbent to exhibit high selectivity and capacity for carbon dioxide over these bulk gas components.
3) Kinetics of adsorption: Fast adsorption (and desorption) kinetics is essential for an efficient system. Adsorption/desorption kinetics control the cycle duration of the system. This value is determined by the reaction kinetics of carbon dioxide with the functional groups in the sorbent. Faster an adsorbent can capture CO_2, less amount of it is required.
4) Mechanical strength: Microstructure and morphological stability should be provided by the sorbent during multi-cycling between adsorption and desorption steps. Operating conditions of the system such as pressure, temperature, vibration, high volumetric flow rate and high pressure change should not cause any significant fluctuations in the adsorbent's structure.
5) Chemical stability: For carbon dioxide capturing systems, sorbents should be able to remain stable in an oxidizing environment and be resistant to contaminants in the gas stream such as SO_x, NO_x and heavy metals. It is preferred to remove these components before the adsorption step, but in case of missing this part, sorbent has to be able to tolerate this situation [16].
6) Regeneration: A good candidate for CO_2 capturing should be regenerable in order to have an effective structure. This aspect of the sorbent during

repeated steps of adsorption and desorption steps can also reduce the costs of the whole process.

7) Cost: It is perhaps the most delicate characteristic. The costs per kilogram of synthesizing sorbents is one of the first things come to mind. Comprehensive studies should be done to come up with a price baseline for an economic procedure.

Among the available options, typical sorbents include activated carbon, zeolites and metal organic frameworks (MOF). There are many other candidates such as molecular sieves, mesoporous silica and other carbonaceous materials like graphene or CNTs, but due to inability to meet the explained criteria they are not as popular and practical as the first three materials.

1.2.1. Zeolites

Zeolites are a class of microporous crystalline framework materials which are traditionally used in wide ranges from gas separation to purification. These materials are based on silicate frameworks including the substitution of some part of a silicon atom with aluminum or other metal atoms. This substitution leads to a negative charge with cations, normally by sodium or alkaline metals, inside a pore structure [8]. Due to the crystalline structures, zeolites have uniform pore sizes between 0.5 to 1.2 nm which makes them a good candidate for separating molecules [17]. The mechanism which is used by zeolites for separation of gases is selective adsorption of molecules with a large energetic dipole and quadruple. Carbon dioxide, with high quadrupole moment of -14.29 e-40 $C.m^2$, makes a strong interaction to the electric field of cation structure in zeolites [18]. The factors which affect gas adsorption on zeolites are the structure of framework, the composition of the framework, size of molecules, shape of molecules, purity, polarity and cationic form.

Zeolites show a promising capacity for CO_2 adsorption from a gas stream. Many studies have been conducted and published regarding CCS process on different types of zeolites such as types A, X and Y or natural zeolites such as chabazites, clintopiles and mordenites. Siriwardane et al. showed that natural zeolites with higher sodium content bring higher adsorption capacity and rate of adsorption [19]. Unfortunately, kinetic studies of CO_2 adsorption, which is an important factor as discussed before, on zeolites

are rarely reported. Investigations on erionite (ZAPS) indicated that adsorption process on this sample occurs very fast and about 70% of total capacity is achieved at both 0 and 20 °C [20]. Moreover, it has been reported that water has a harmful effect on carbon dioxide adsorption. Water molecules competitively adsorbed on the zeolite's surface and block the access to other gases, ergo even small amount of H_2O reduces zeolite's capacity for carbon capture, dramatically [21].

To put it in a nutshell, carbon dioxide adsorption on zeolites has a fast kinetics compare to other sorbents and equilibrium capacity is reached in few minutes. However, zeolite's carbon capture is highly affected by the process temperature and pressure. The adsorption capacity drops significantly by increasing temperature, as well as gas-phase partial pressure. Also, the presence of water molecules in the flue gas stream limits the application of zeolites by reducing the capacity.

1.2.2. Metal organic frameworks

Metallic vertices strongly connected by organic linkers comprise the structure of metal organic frameworks (MOFs). These adsorbents have narrow and controlled pore size distribution in the molecular-size region. The ability to vary linkers results in having various options to control size and shape of the pores, and chemical potential of the surface which affects the kinetics, capacity and selectivity. This flexibility in shape and size has led to more than 20,000 different MOFs synthesized and studied; their surface area is reported in a range of 1000 to 10,000 m^2/g [22]. The popularity of MOFs is due to their selectivity high adsorption capacity, particularly for H_2 and CH_4 adsorption.

Although MOFs are principally a good candidate for CCS, still choosing useful MOF materials for implementation purposes is challenging. The flue gas stream from fossil fuel combustion contains 15 to 16% of CO_2 and high content of N_2. In the ambient pressure of 1 atm, this leads to low partial pressure for carbon dioxide. Metal organic frameworks have considerably high capacity for carbon dioxide capture. However, at a low partial pressure of CO_2, they exhibit a poor capture performance compare to the other adsorbents [23]. Unfortunately, maintaining high partial pressure is not economic, process unit costs wise. Furthermore, synthesis of a MOF, a metallic complex with organic ligands, is very expensive in many cases, and the process is complicated [7].

Despite the high surface area in MOFs, they suffer from mechanical strength and durability issues. The moisture in the gas stream has fatal impacts on the structure of

MOF, therefore its application in power plants is limited [24]. Additional studies are required to develop MOFs targeting the key properties discussed, such as stability, multicycle applicability and competitive selectivity.

1.2.3. Activated carbons

To have a simple definition, activated carbon (AC) is a carbonaceous, highly porous adsorptive medium that has a complex structure composed primarily of carbon atoms. Activated carbons are carbonaceous crystalline sorbents. They are available with a wide range of properties, depending on the raw material and activation method [14]. Samples produced from coal, petroleum and biomass are widely used in different industries e.g. gas separation, purification and water treatment. Different precursors, carbonization methods and activation steps have been used by manufacturers and scientists to provide a large variety of ACs for gas separation, especially carbon capture and adsorption.

By controlling the preparation, carbonization and activation condition, the pore structure of ACs can easily be controlled. Likewise, functional groups on the surface of activated carbon can also be controlled by different treatments, or using different raw materials [25]. Based on the precursor which the activated carbon is produced of, the pore size distribution of them varies from micropore to macropore [23]; therefore it is not appropriate to recommend whole activated carbon species for selective adsorption of a specific gas. Pore size distribution of AC is highly influenced by morphology and structure of the source material. Activated carbon's morphology is dependent to microcrystalline graphite components stacked in random orientations that allow the microporous area to form [8]. According to Ruthven, AC samples produced from coconut shell are mainly micropore materials, although peat based ACs are mainly macroporous. Surprisingly, different types of lignite translate to different types of AC with pore size distribution from mesopore to macropore areas [26].

Engineering pore size distribution of AC and its effect on CO_2 separation is being studied over years. Oschatz and Antonietti showed that pore size distribution has major effects on the selectivity of CO_2 on the samples [10]. Not only it is favorable to have microporous material for carbon capturing process, as discussed, but also the size of these micropore areas is a key element. To have the highest pick in carbon dioxide uptake it is

better to have pores with a size of 0.5 to 0.7 nm or even lower, which are referred to as ultra-micropores.

According to the previous studies, ACs are one of the best options for CO_2 capture. Activated carbons have low production costs and their structure would not be damaged or changed in the presence of moisture. They have a high surface area, and also CO_2 adsorption capacity. This material has relatively better thermal and mechanical stability and can endure working conditions of CCS systems [25].

ACs can be produced both chemically and physically. In physical activation, the carbonized raw materials go through one or more heat treatments. Heating in high temperatures eliminates tar-like structures from the sample and exposes the porous area within [27]. While in chemical activation, the carbonized materials are mixed with an agent to increase the porosity. ACs have been successfully produced via various agents such as H_2SO_4, HCl, $ZnCl_2$ and H_3PO_4. Recent attempts to use alkali hydroxide i.e. KOH and NaOH as the activation agents exhibit high specific surface areas [28]. Chemical activation of AC has been reported as more advantageous over physical activation due to higher yields, more surface area and better development of porous structures in carbon [29].

Many researches have been carried out and reported on different aspects of CO_2 adsorption on activated carbon. Saxena et al. derived a parametric analysis on a practical model of a simple CCS configuration [30]. They studied the effect of some key parameters of the system such as the initial temperature of the system, diameter of the chamber and temperature of the cooling fluid. Their results showed that narrower chamber size and colder working conditions, improve the CO_2 adsorption efficiency.

Singh and Kumar modeled the isotherms for CO_2 adsorption on commercial activated, lignite based granular materials, via Langmuir and Dubinin-Astakhov isotherm models [5]. They indicated that the Dubinin-Astakhov model is the most suitable for CO_2 capture on AC. Another important result of their study was that according to their data, it is determined that CO_2 adsorption is physisorption process and it is an exothermic and spontaneous phenomenon. However, work of Guo et al. specified that not necessarily all AC samples follow the same equation for their carbon dioxide adsorption. A part of their samples followed the Dubinin-Astakhov model while the other samples had isotherms compatible with Freundlich equation [31].

As explained before, basic raw material and synthesis conditions and materials translate into a wide range of diversity in activated carbons. Therefore, there are numerous researches and studies done on activated carbons. The effect of different aspects of production depends not only on their structure and characteristics, but also on their performance as an adsorbent for carbon dioxide capturing objectives. Additionally, studying the isotherms of CO_2 adsorption for different AC samples help to develop an efficient, competent and economic carbon capture and storage system. It should be mentioned that operating elements and conditions of the adsorption system have critical effects on its capacity and efficiency, but examining those parameters are not current study's concern.

1.2.3.1. Biomass based activated carbon

As discussed above, activated carbon can be produced from different precursors. A typical material of choice is coal, but recently, attempts to synthesize AC from biomass have been significantly increased. It is determined that usually the AC from biomass provides higher surface area and more microporous zones, mentioned in the previous section, which is favorable for carbon dioxide capture. Compared to non-renewable coal-based granular samples, ACs obtained from biomass sources especially from agricultural side products bring more advantages, such as better efficiency and lower production costs. Biomass is one of the most abundant materials on earth. This availability makes by-products of the agricultural industries a perfect raw material for AC synthesis.

In recent years, introducing waste materials from industry and agriculture as an alternative substance for AC production has become a growing research interest. An important challenge in synthesizing activated carbon in commercial scale is to find a suitable precursor that is cheap, hence the focus on biomass based AC production has been incomparably raised [29]. The agricultural waste, chosen for AC, differs by the agricultural industry in the designated region. Depending on the products, the precursor can be selected from corn hub, coconut shell, orange peel, nuts' shell, crops' pith, wasted tree branches and so many other options. Each region can have its own choice of raw material.

Orange peel was chosen as a low-cost precursor and activated with zinc chloride and potassium carbonate, and later the sample's structure and adsorption properties were studies by Köseoğlu and Başar [29]. The results reveal that, AC sample activated by

$ZnCl_2$ had lower BET surface area and lower yield. Both samples were heterosporous with micropore areas. Williams and Reed activated flax fiber both physically and chemically, by zinc chloride [32]. Chemically activated samples had three times more surface area than physically activated ones. Also, physical activation only produced a mesoporous structure, while chemical activation led into manly microporous regions, which was an interesting outcome of this study.

Ribs et al. compared activated carbon produced from cocoa shell with commercial samples in adsorption of violet dye [33]. They used a mixture of inorganic components (red mud + lime + Na_2SO_4 + KOH + $Al(NO_3)_3$) as the activation agent. In addition to a higher surface area, biomass-based AC samples had incredibly faster adsorption. The equilibrium time for violet 5 dye adsorption was reported as 45 and 150 min for biomass-based AC and commercial AC, respectively.

Many other studies can be mentioned about AC production from different biomass materials such as macadamia nutshell [34], coconut shell [35], soybean oil cake [28], etc. Various biomass sources, diverse activation agent and different carbonization and activation parameter like time and temperature, provide us with infinite kinds of activated carbon. The objectives of each sample differ from each other but they all have one common point, bio-based activated carbons are far more effective than commercially available coal-based activated carbon. Lower production cost, higher surface area and better adsorption performance make bio-based AC more favorable over the other kinds.

1.3. CO_2 adsorption on biomass based activated carbon

Advantages of activated carbon over other adsorbents for carbon capturing were mentioned before. By superior characteristics that bio-based ACs have over the typical models, it seems to be useful to use biomass based activated carbon for separation of CO_2 from the flue gas streams. Many studies and tests have been conducted for this purpose [36, 37].

Gonzalez et al. activated olive stones and almond shells for CO_2 adsorption and investigated the synthesized samples' adsorption performance in two different temperatures of 25 and 100 °C [38]. Their results showed that increasing time of activation first, decreased the yield percentage, and second increased the CO_2 uptake. Moreover, adsorption performance of ACs dropped dramatically by increasing the adsorption temperature, which was predicted from the Langmuir isotherm equation. This

group found out that the Dubinin-Astakhov model agreed better for their samples. An interesting result of this study was that CO_2 uptake is constant for AC samples of different activation time, and this parameter does not have any effects on the capacity at higher temperatures.

Effect of micropore and mesopore structure of biomass based AC on carbon adsorption was investigated by song et al. [39]. The same activation method of Gonzalez work was carried out on corn stalk, following by a chemical activation step via HNO_3, KOH and CH_3COOH at two different time and temperatures. Their study revealed that the additional chemical activation steps modified the structure and performance of physically activated samples. The maximum carbon uptake and surface area had belonged to the samples activated by nitric acid at a higher temperature and longer activation duration time. Furthermore, their result indicated that biomass based activated carbon has much better adsorption performance over commercial models.

In another study, Singh and Kumar measured the CO_2 adsorption pressure concentration isotherms for activated carbons based on coconut shell [40]. The outcomes were a conclusion for their previous works. Once again, they concluded that CO_2 adsorption on their samples follows Dubinin equation and the adsorption capacity drops by increasing the process' temperature, as expected.

Among the numerous studies about carbon dioxide adsorption on biomass based activated carbon it can be indicated that these kinds of ACs are the best candidate for carbon capture purposes. Despite the differences due to precursors and activation methods, all bio-based AC samples have shown better performance than the commercially available samples. Moreover, low cost of production of these materials cannot be ignored. Higher selectivity and durability of activated carbons are discussed previously and there is no need to mention them again. All these and more, make bio-based AC a perfect sorbent for CO_2 adsorption for flue gas stream from power plants or industrial sites.

Present work

In this study, sunflower pith from a local farm was chosen as the biomass precursor from an agricultural waste. The activation process was a combination of both chemical and physical activation. First the biomass was mixed with the activation agent, potassium hydroxide (KOH) or sodium hydroxide (NaOH), and then thermally treated. Structural characteristics of the synthesized activated carbon were analyzed by different tests. Nevertheless, the objective of this research was to use biomass based activated carbon in carbon dioxide adsorption. The adsorption performance and capacity of the produced AC were investigated by the evaluation of their adsorption isotherms.

It is important to see if this local biomass material is suitable for carbon capture and storage processes, and if so it should be investigated to find a "sweet spot" for carbonization and activation steps. Also, a commercial type of AC was used in this study to compare the performance and characteristics of the produced models to the available ones on the market.

In the next chapter, materials and the synthesizing process are explained thoroughly. Every step from the preparation of the biomaterials to conducting the tests are explained and clarified. Afterward, at chapter 3, results of all tests are presented and discussed. It has been tried to define every outcome from the tests and experiments. At the end the CO_2 adsorption capability of the produced samples will be reviewed.

CHAPTER 2

2. MATERIALS AND METHODS

2.1. Experimental

2.1.1. Materials

As mentioned above, the raw material for the activated carbon production was the sunflower pith which is a part of agricultural residues in the respective section. The pith was provided from a farm in Düğüncülü village, at the suburban of the city of Kırklareli, northwestern Tukey.

The activation agents for chemical activation step in this study were potassium hydroxide (KOH), from Merck KGaA (M = 56.11 g/mol), and sodium hydroxide (NaOH), purchased from Sigma-Aldrich (M = 40 g/mol, purity 98-100.5%). The reason behind choosing these two alkali hydroxides is their advantages over other agents. The alkali hydroxides, KOH and NaOH specifically, are more available, cheaper and safer than other traditional options for chemical activation such as nitric acid (HNO_3) and sulfuric acid (H_2SO_4) [41, 42]. It is expected that for the chosen raw biomass material in this project, NaOH translates to a higher surface area and better structure over KOH [34]. But also it is reported that NaOH is effective for low structural-ordered materials, while KOH works better in activating higher ordered substances [28]. One of the objectives of this study is to investigate the better agent for the chemical activation process.

Moreover, a commercially available activated carbon sample was provided from Merck KGaA (M = 12.01 g/mol) to compare the structural properties, functional groups and adsorption capacity of the synthesized samples. It is important and useful to compare the performance of the produced ACs to a coal-based commercial one.

2.1.2. Carbonization and Synthesis of Bio-Chars

The preparation, carbonization and activation processes applied here was based on the works of Cazzeta et al. [35] who investigated the adsorption of methylene blue on NaOH activated carbon from coconut shell. This activation process consists of both physical and chemical steps together which leads to better and higher quality AC samples, as it is reported.

The AC production procedure was as follows:

1. Preparation and drying: The sunflower pith, the biomass precursor, was peeled after drying and the inner foam like cores, Figure 4, were collected.

2. Grinding: Peeled sunflower pith was ground and meshed to have bioparticles with a size of 1 mm, Figure 5.

Figure 4. Sunflower's pith before and after peeling

Figure 5. Ground and meshed sunflower pith.

3. Carbonization: The powdered biomass precursor was heated with 10 °C/min heating rate inside a neutralized environment by nitrogen. Four different temperatures of 350, 400 450 and 500 °C were considered as the target carbonization temperatures. For the carbonization duration, the

process was done in 30, 60 and 120 min. The resulting bio-chars were stored inside a sealed area for the further analyses and activated carbon production.

It has to be mentioned that bio-chars produced at 350 and 400 °C had a brownish color, Figure 6, unlike the samples from higher temperatures or commercial char-coals which were completely black. Shorter carbonization led to a lighter brown color. This color difference was probably due to uncomplete carbonization on the biomass' structure. Characteristics of all samples will be presented and discussed later, at the following chapter.

Figure 6. Brown color appears in carbonization at 350 °C

For an easier referring, the produced bio-chars were labeled as the terms in Table 1. Due to the reasons which will be explained in the next chapter, BC-11 and BC-12 showed better qualities and appeared to be more efficient options to produce activated carbon, ergo they were chosen for AC production

Table 2. Synthesized bio-char labeling

Duration [min] \ Carbonization Temperature [°C]	350	400	450	500
30	BC-1	BC-4	BC-7	BC-10
60	BC-2	BC-5	BC-8	BC-11
120	BC-3	BC-6	BC-9	BC-12

2.1.3. Synthesis of bio-based activated carbons

4. The Chosen bio-chars were mixed with 3:1 mass ration (agent: bio-char) of KOH or NaOH, and enough distilled water to make the mixture slurry, for 2 hours.
5. The mixture was dried at 130 °C for 4 h, via an oil bath heating.
6. The dried mixture was heated from room temperature to 700 °C, with 10 °C/min heating rate, inside a neutral environment provided by nitrogen.
7. After cooling, the remaining was washed with 0.1 M hydrochloric acid solution following by hot distilled water till reaching to pH 6.5-7.5.
8. The obtained carbon was dried at 110 °C for 24 h and then kept inside closed containers for further analyses, Figure 7.

Figure 7. Synthesized biomass-based activated carbon.

The ACs were labeled as below (Table 3). It is reported that NaOH is more effective in activating low structural ordered materials, while KOH is more efficient in case of the highly ordered materials, which results in differences in the performance of samples activated by both hydroxides [28].

Table 3. Synthesized activated carbon labeling

		Agent	
		KOH	NaOH
Bio-Char	BC-11	AC-1	AC-3
	BC-12	AC-2	AC-4

2.2. Characterization

Textural characterization of all materials i.e. raw biomass, bio-chars and ACs were carried out by 77 K nitrogen adsorption and desorption using Micromeritics 3Flex Surface Characterization device. The surface area, S_{BET}, was calculated via isotherms from the Brunauer–Emmett–Teller equation (BET), in the range of relative pressure from 0.03 to 0.1. The total pore volume was defined as the volume of liquid nitrogen corresponding to the amount adsorbed at a relative pressure up to P/P0 = 0.99 [29]. Dubinin-Radushkevic equation was used to determine the micropore volume. The average pore diameter, was calculated by the DFT method.

Thermogravimetric analyses and ash content determination of biomass material and bio-chars were implemented by NETZSCH Simultaneous Thermal Analyzer STA 449 C Jupiter, a heating rate of 10 °C/min. Fourier Transform Infrared (FTIR) spectroscopic analysis of all samples was performed using a Thermo Scientific's Nicolet iS10 FT-IR spectrometer, in wavelength between 4000 to 500 cm^{-1}. Also, the surface morphology of the synthesized samples was observed using LEO Supra VP35 field emission scanning electron microscopy.

2.3. Carbon dioxide adsorption

Using Hiden Isochema IGA-001 Gravimetric Gas Sorption Analyzer, CO_2 adsorption tests were performed on the bio-based synthesized activated carbons. Isotherms from this test were recorded in pressures from 0 to 9 bar, at room temperature. Figure 8 shows the schematic diagram of the gravimetric adsorption analyzer [43].

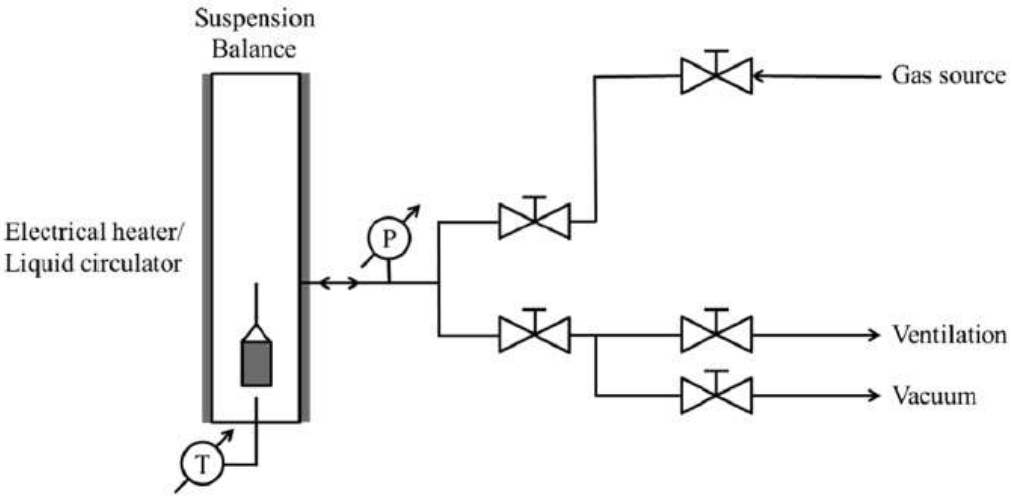

Figure 8. Schematic diagram of the gravimetric gas adsorption analyzer

CHAPTER 3

3. RESULTS AND CONCLUSION

3.1. Results

3.1.1. Yield

The bio-char's yield was defined as the final weight of product char after carbonizing at the target temperature and time. This yield percentage was determined by the relation below [35]:

$$Yield_{BC} = \frac{w_{BC}}{w_0} \times 100$$

where w_{BC} and w_0 are the final produced bio-char and the dried precursor's weight, respectively. The values calculated for this study are shown in the Table 4.

Table 4. Yield percentage for bio-chars

	BC-1	BC-2	BC-3	BC-4	BC-5	BC-6	BC-7	BC-8	BC-9	BC-10	BC-11	BC-12
Yield [%]	43.66	42.69	41.26	40.09	38.98	37.24	38.06	37.19	35.74	34.39	33.77	32.58

From Table 4 it is concluded that by increasing the time and temperature of the carbonization process, the yield decreases, which was expected from the literate [35, 44]. As mentioned in the previous chapter, BC-11 and BC-12 were chosen for the activation process. One of the reasons for this decision was close yield value of these two bio-chars which brings out this assumption that they probably have similar characteristics to each other. This phenomenon can be seen better by the thermogravimetric tests, illustrated in Figure 9.

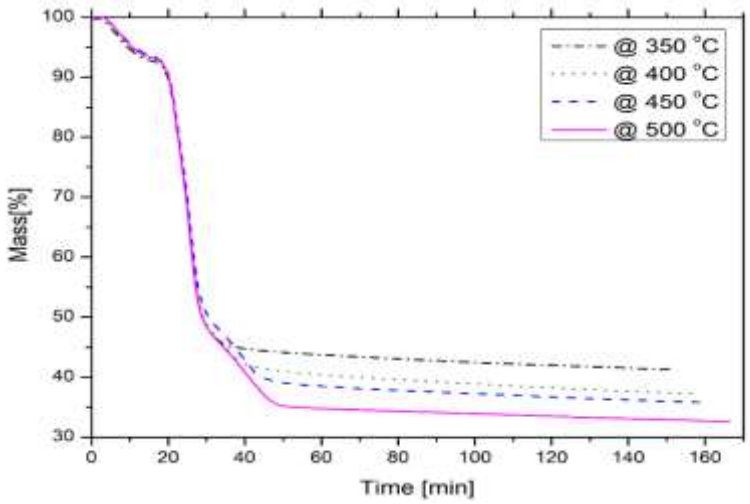

Figure 9. Effect of carbonization time and temperature on yield percentage

The yield for the produced ACs was also determined same as bio-chars.

$$Yield_{AC} = \frac{w_{AC}}{w_0} \times 100$$

which w_{AC} represent the weight of the AC after activating, washing and drying. The yield values for ACs were 27.34%, 25.47%, 18.68% and 17.4% for AC-1, AC-2, AC-3 and AC-4, respectively. According to the results, applying NaOH as the activating agent instead of KOH brings a decrease in the values of yield percentage. This is justified by the action of the agent (NaOH), which provided elimination and dehydration reactions, breaking the bonds C–O–C and C–C of the raw material [35, 45].

3.1.2. Ash Content

Analyses for the ash content of the bio-chars are illustrated in Figure 10. By using TGA test and heating the samples from room temperature to 1000 °C in presence of air (dry combustion), the amount of mineral and other inorganic matters is within the bio-char samples can be determined [27].

The first mass reduction in this test, which happens at about 100 °C, is due to the water molecules which left the surface of the samples at that temperature. The next main step of mass reduction between 200 to 600 °C belongs to combustion of the carbon within the samples. The remaining ash after this combustion is the mineral and inorganic content of produced bio-chars.

The first point that is noticed on these graphs is that for the samples produce at 500 °C mass reduction during dry combustion happens in one step and graph is simpler than the results belong to other samples. This is because of elimination of functional groups of biomass material. It was expected that by increasing the carbonization temperature, more functional groups vanished from the precursor. Functional groups of sunflower pith, bio-chars and AC will be discussed thoroughly at the next section, but it should be mentioned that from the TGA results for the ash content, it can be determined that increasing the carbonization temperature translates to higher quality of produced bio-chars.

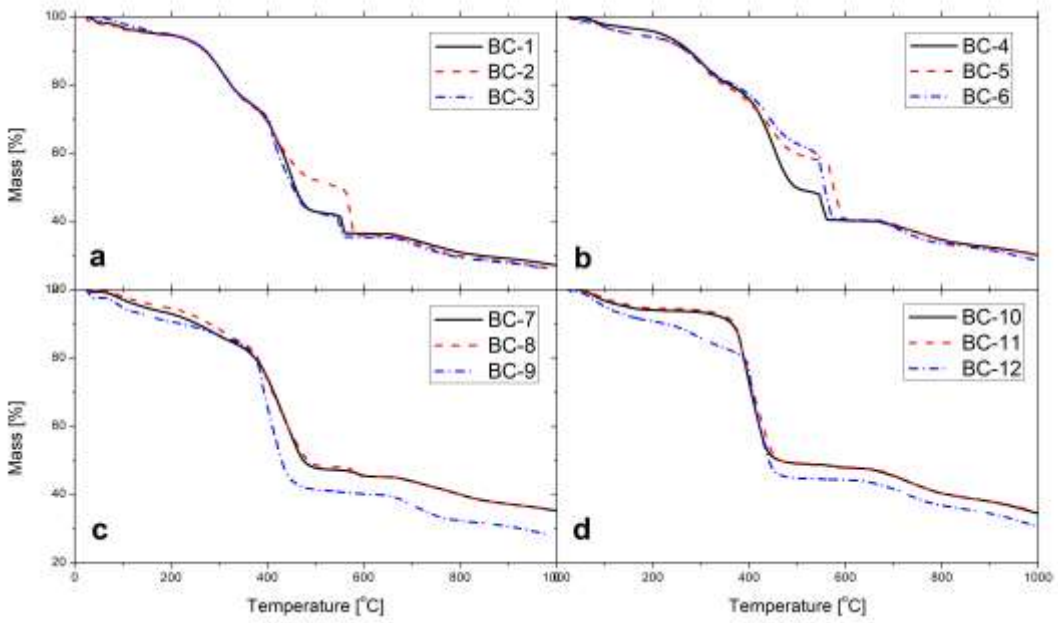

Figure 10. Ash content of bio-chars produced at a) 350 °C, b) 400 °C, c) 450 °C, d) 500 °C

Carbonization duration does not have any noticeable impact on ash content of the samples. The values of the ash content of the bio-chars were measured as 58.68, 54.14, 46.75 and 45.51% at 350, 400, 450 and 500 °C carbonization, in that order. By increasing the pyrolysis temperature more of the minerals in the biomass were eliminated and again it was another proof of advantage of carbonization at a higher temperature. An energy dispersive X-ray spectroscopy (EDA) test on the powdered sunflower pith detected traces of calcium (Ca), magnesium (Mg), chlorine (Cl), potassium (K) in its structure, Figure 11, which are the content of the remaining ash.

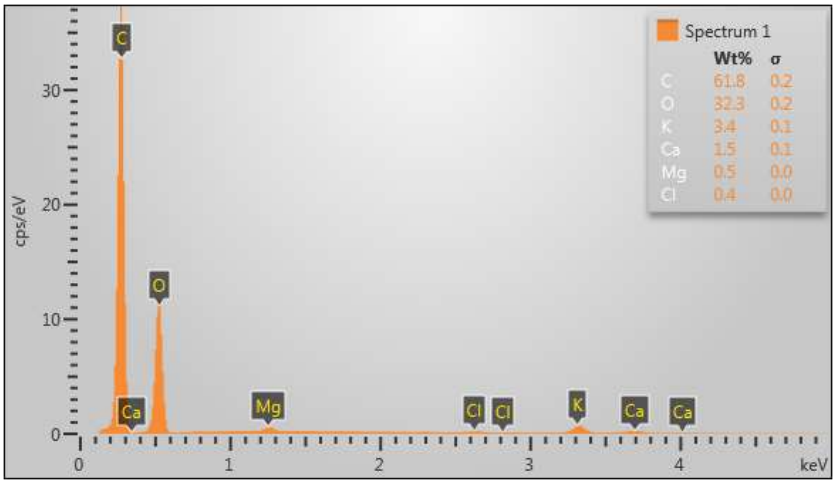

Figure 11. Energy dispersive X-ray spectroscopy (EDA) of sunflower pith.

3.1.3. Functional Groups

The functional groups which were identified from the FTIR spectrum for the biomass and biochar samples are presented in Tables 5 and 6 [29, 44]. These spectra are also shown in Figure 12 and 13.

In the spectrum for the sunflower's raw sample, the broadband of O-H stretching at the 3300 to 3000 cm^{-1} range specifies the oxygen-containing functional groups in the organic matrix of the biomass structure [46].

Table 5. Functional groups of biomass sample determined by the FTIR

Wave Numbers [cm^{-1}]	Functional Groups
3331.41	–OH Stretching
2902.7	Aliphatic CH Stretching Vibration
1597.72	Aromatic C=C Ring Stretching
1415.53	Aromatic C=C Ring Stretching
1317.58	Aliphatic CH_3 Deformation
1202.57	Aromatic CO– Stretching
1021.88	Aliphatic Ether C–O and Alcohol C–O Stretching
893.81	Aromatic Ring

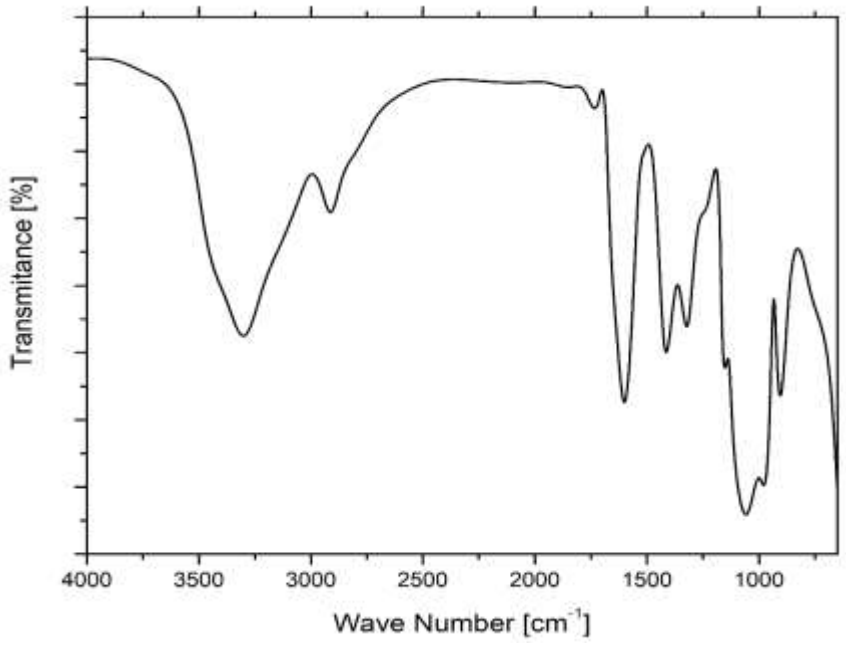

Figure 12. FTIR spectra of the biomass sample

Table 6. Functional groups of biochar samples determined by the FTIR

Wave Numbers [cm^{-1}]			Functional Groups
30 min	60 min	120 min	
350 °C			
3331.23	3331.19	3332.7	–OH Stretching
2926.86	2925.57	2928.74	Aliphatic CH Stretching
1559.73	1558.86	1559.48	Aromatic C=C Ring Stretching
1405.6	1406.04	1402.15	Aliphatic CH_3 Deformation
1313.55	1314.56	1315.41	Aromatic CO – Stretching
1128.15	1130.87	***	Aromatic CO – Stretching
864.97	865.06	865.57	1 adjacent H deformation
780.04	780.97	779.89	2 adjacent H deformation
400 °C			
3166.14	3190.15	3337.66	–OH Stretching
2924.83	2923.52	2928.57	Aliphatic CH Stretching
1555.52	1556.38	1565.6	Aromatic C=C Ring Stretching
1402.62	1405.34	1396.69	Aliphatic CH_3 Deformation
1124.84	1123.14	***	Aromatic CO – Stretching
869.64	869.12	868.27	1 adjacent H deformation
781.4	780.97	780.89	2 adjacent H deformation
450 °C			
3039.93	3048.49	3161.41	–OH Stretching
1405.55	1406.55	1384.22	Aliphatic CH_3 Deformation
1119.64	1119.59	***	Aromatic CO – Stretching
869.52	869.24	868.24	1 adjacent H deformation
749.45	746.59	747.53	2 adjacent H deformation
500 °C			
3200.8	3172.53	3162.07	–OH Stretching
1394.43	1376.23	1382.6	Aliphatic CH_3 Deformation
871.09	869.59	868.76	1 adjacent H deformation

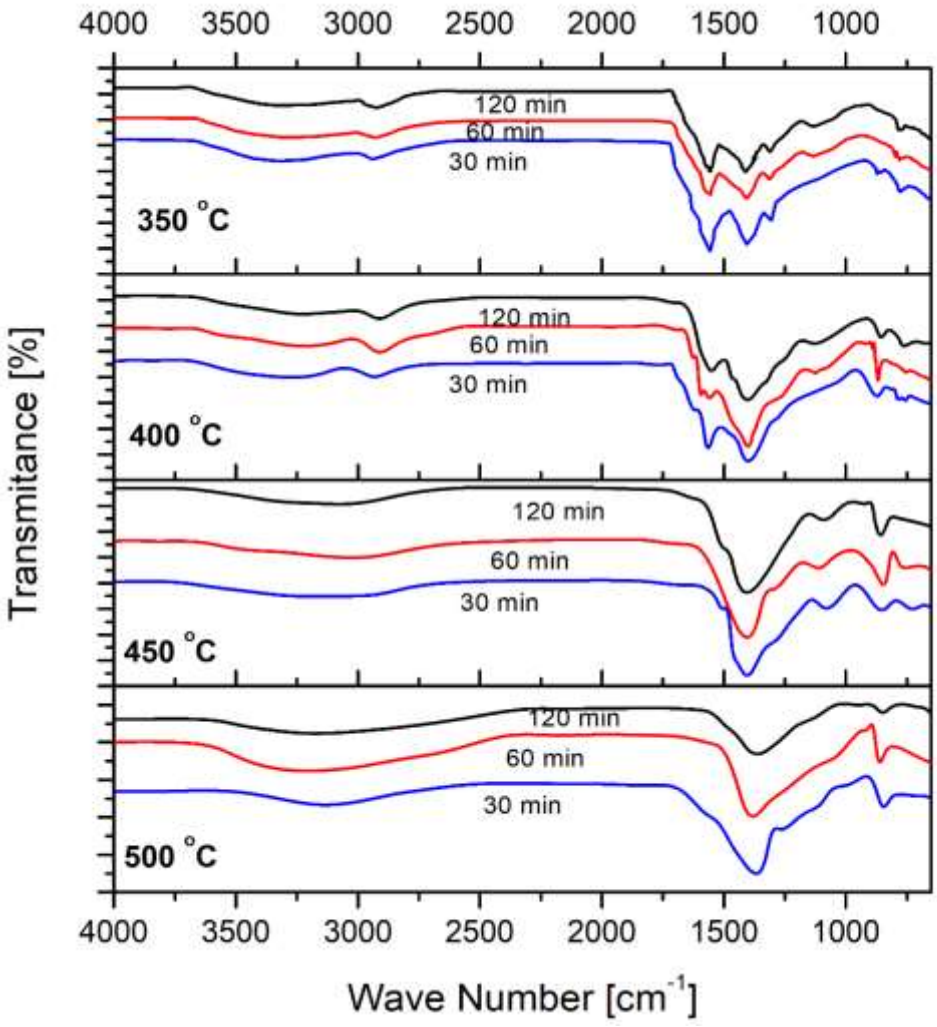

Figure 13. FTIR spectra for the biochar samples

During the carbonization, by increasing the process' temperature, most of the functional groups of the precursor were diminished. The FTIR spectra of the bio-chars BC-7 to BC-12 (450 °C and 500°C pyrolysis) shows a loss for most of the functionalization in the region from 3500 to 1600 cm^{-1}. Aliphatic CH stretching around 2900 cm−1 also diminished due to complete removal of hydrogen containing aliphatic groups [47]. The peak around 1550 cm^{-1} for BC-1 to BC-6 (350 °C and 400 °C) is an indication that the aromatic structure was still preserved after the carbonization at the designated temperatures, although their intensity decayed. The aromatic CO stretching bands between 1300 and 1050 cm−1 mostly associated with the plant's cellulose structure [27]. They lost their intensity after carbonization by increasing the temperature

of the process and perished at 500 °C which once again approves the impact of carbonization temperature on the quality of the produced bio-char.

Unlike the temperature, time didn't have a significant effect on the functional groups; although it should be mentioned that for 120 min carbonization an aromatic CO stretching vibration was removed from the biomass. This poor impact of time was another reason to consider BC-11 along with BC-12 as an option for the activation step.

The spectra and the functional groups for activated carbons are shown in Table 7 and Figure 14. Results followed very similar trends. Because of the activation process, chemical bonds were broken, and most of the functional groups were lost. The most distinct difference between bio-char and AC was the disappearance of 1400 cm^{-1} peak, related to the aliphatic groups. This could be the result of decomposition of lignin part in the char during activation which was conducted at 700 °C [48].

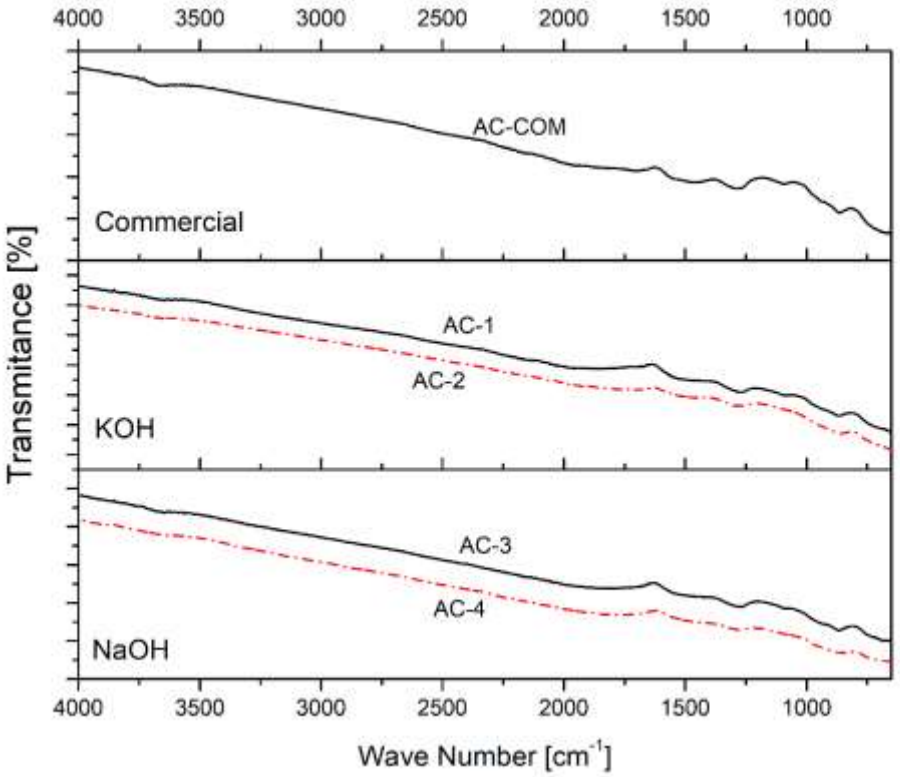

Figure 14. FTIR spectra for the AC samples

As explained before, for comparison reasons, a commercial AC sample, AC-COM, also got analyzed along with the produced ones. It is seen that the functional group in both synthesized ACs in this study and commercial materials available in the market show the same pattern in the FTIR spectra. However, in AC-COM, two bands of

carboxylic groups and asymmetric stretching of C-O-C appears, which are related to their synthesis conditions.

Table 7. Functional groups of AC sample determined by the FTIR

Wave Numbers [cm^{-1}]				Functional Groups
AC-1	AC-2	AC-3	AC-4	
1850.83	1704.86	1764.60	1841.64	C=O Stretching
1264.43	1271.79	1271.10	1267.81	C–O–C Stretching
862.35	861.74	864.9	865.75	Aromatic C–H Ring Stretching
AC-COM				
1694.01				C=O Stretching
1460.65				C=O Stretching in Carboxylic Groups
1287.23				C–O–C Stretching
1095.19				C–O–C Asymmetric Stretching
860.66				Aromatic C–H Ring Stretching

3.1.4. Textural Characterization

The porous structure of the bio-char and AC samples were determined by obtaining nitrogen adsorption isotherms at 77 K. These isotherms are illustrated in Figure 15 and 16. For the bio-chars, the graphs show that they vaguely follow the type II isotherms. This indicated microporous characteristics of the chars and probably a multilayer formation of adsorbent on the adsorbate [44].

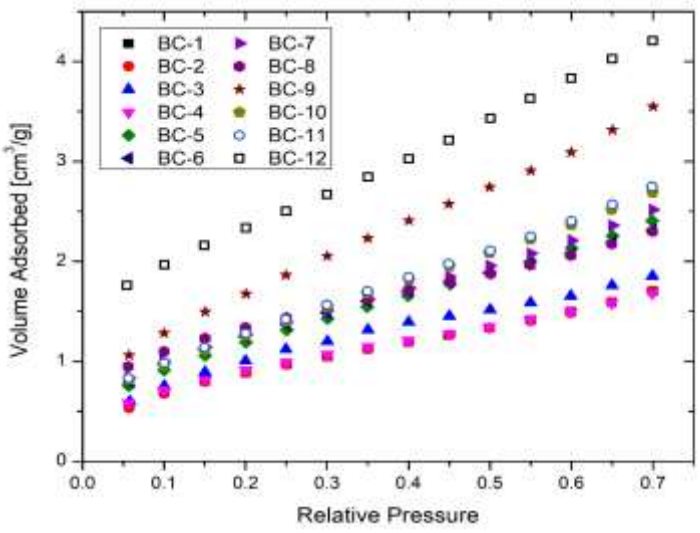

Figure 15. Adsorption isotherms of N2 at 77 K for bio-char samples

The calculated BET surface area for the bio-char samples are presented in Table 8. As expected, increasing the temperature and time of carbonization process led to higher surface area values. These results are another reason to pick BC-11 and BC-12 as precursors for activation. Of course, BC-12 is a more favorable candidate for activation process, from all aspects of yield percentage, functional group, and surface area, but preparing BC-11 took half of the time of preparation of BC-12. Synthesizing an AC with the best characteristics possible is the objective of this research and many others, but the efficiency with time and energy saving should be taken into account as well.

Table 8. BET surface area for bio-char samples

	BC-1	BC-2	BC-3	BC-4	BC-5	BC-6	BC-7	BC-8	BC-9	BC-10	BC-11	BC-12
S_{BET} [m^2/g]	3.44	3.51	4.11	3.52	4.67	4.9	4.87	4.92	5.06	4.98	5.11	5.35

About the activated carbon samples, according to Figure 16, the isotherms are mainly consisting of type I and for higher relative pressures, of type II. The type I isotherm, which is also known as Langmuir, indicated that the adsorbent and adsorbate have high affinity, and the analyzed materials, here activated carbon, mostly consist of micropores [49]. The steep slope of the diagram before low pressure, before the relative pressure of 0.1, determines a wide range of micropore distribution.

Moreover, the steady area over 0.1 for the samples AC-1 and AC-2 expresses more Langmuir behavior of ACs activated by KOH, rather than NaOH; despite of the higher adsorption [48]. The micropore area of low-pressure region follows by a mesopore filling at high pressure, demonstrated by type II isotherm [34]. In one way or another, the samples activated by NaOH brought much higher and wider porosity range, micropore and mesopore, than KOH activated samples.

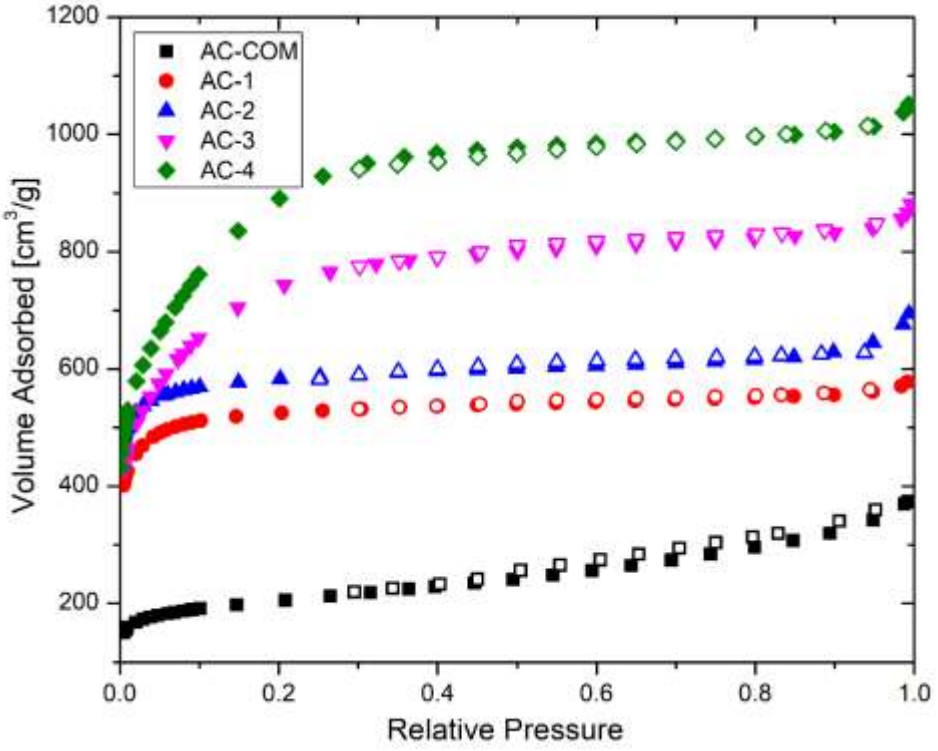

Figure 16. Adsorption and desorption isotherms of N2 at 77 K for activated carbon samples

The results for porous texture analysis of AC samples are presented in Table 9, where S_{BET}, V_T, V_μ, V_m and D_P are the BET surface area, total pore volume, micropore volume, mesopore volume and average pore diameter, in that order. These results are affirmations for the isotherm analysis. First, it got cleared that longer carbonization duration results in higher surface areas for the activated carbons. Increasing the carbonization time from 60 to 120 min triggered 7.00% and 10.90% growth in KOH and NaOH activated samples, respectively. Same behavior was seen about the pore volumes.

Table 9. Textural characteristics of the activated carbons

	S_{BET} [m^2/g]	BET P/P_0 range	C constant	V_T [cm^3/g]	V_μ [cm^3/g]	V_m [cm^3/g]	V_μ/V_T [%]	D_P [nm]
AC-1	2109.17	0.05 – 0.1	847.38	0.91	0.69	0.22	0.75	2.17
AC-2	2267.52	0.05 – 0.1	191.31	1.09	0.83	0.26	0.78	2.08
AC-3	2657.73	0.05 – 0.2	117.21	1.21	0.88	0.33	0.69	2.85
AC-4	2948.43	0.05 – 0.2	64.78	1.56	1.07	0.49	0.68	2.63
AC-COM	753.9	0.05 – 0.1	1740.52	0.53	0.18	0.37	0.34	5.81

The specific surface area of the NaOH activated AC-4 was calculated as 2948.43 m^2/g, 24% higher than the KOH activated AC-2 surface area of 2367.52 m^2/g. A wide range of porosity increase was observed in AC-3 and AC-4 surface area due to the combined effect of mesopores and micropores. BET equation is usually applied over the range from 0.05 to 0.2 relative pressures. However, it was observed that usual range was not applicable for KOH activated sample. This is a general situation for microporous samples because of micropore filling is completed at much lower relative pressures [50, 51].

The pore size distribution of the produced and commercial ACs is presented in Figure 17. It is seen that for biomass based ACs majority of the pores were in the microporous and small size mesoporous area, unlike the commercial sample which was mainly contained mesopores. By the Figure 17 it is determined that AC-4, sample activated by NaOH produced from bio-chars with 120 min carbonization, had the highest surface area, but the rate of micropore to total volume for it was lower than other samples. NaOH activation provided higher surface area over KOH, as well as longer carbonization time. However, KOH was the agent that resulted in higher micropore volume rate. This parameter is one the key elements in adsorption and carbon dioxide separation process.

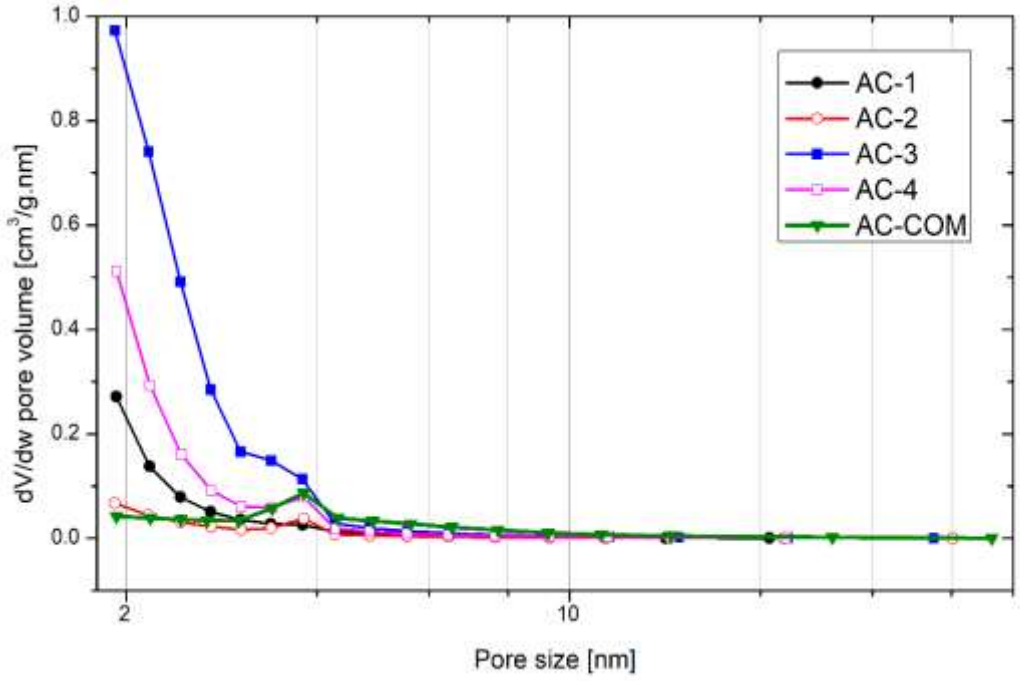

Figure 17. Pore size distribution of AC samples

Moreover. It should be mentioned that the biomass based activated carbon had higher BET surface area than the commercial coal based sample. The smallest surface area difference belonged to AC-1 which was 179.76% higher and in the case of AC-4, the maximum difference of 291.09% increase was recorded. Also, on the bio-based samples, a more microporous area was obtained with respect to the AC-COM which is of high importance in case of adsorption purposes.

Figures 18 and 19 show the SEM analysis of AC-2 and AC-4. The textural characteristic of these samples can be seen in detail here.

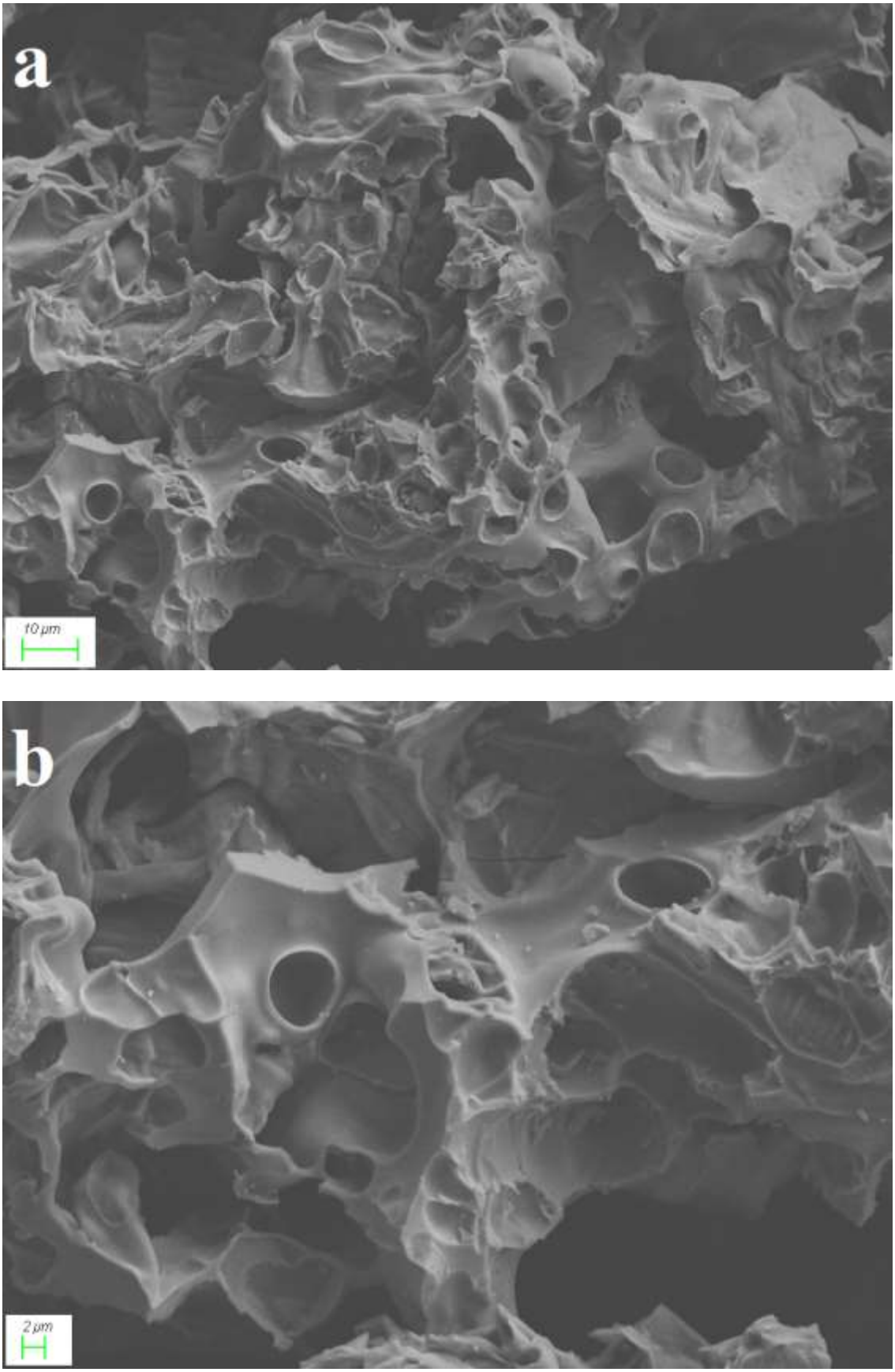

Figure 18. SEM image of AC-2

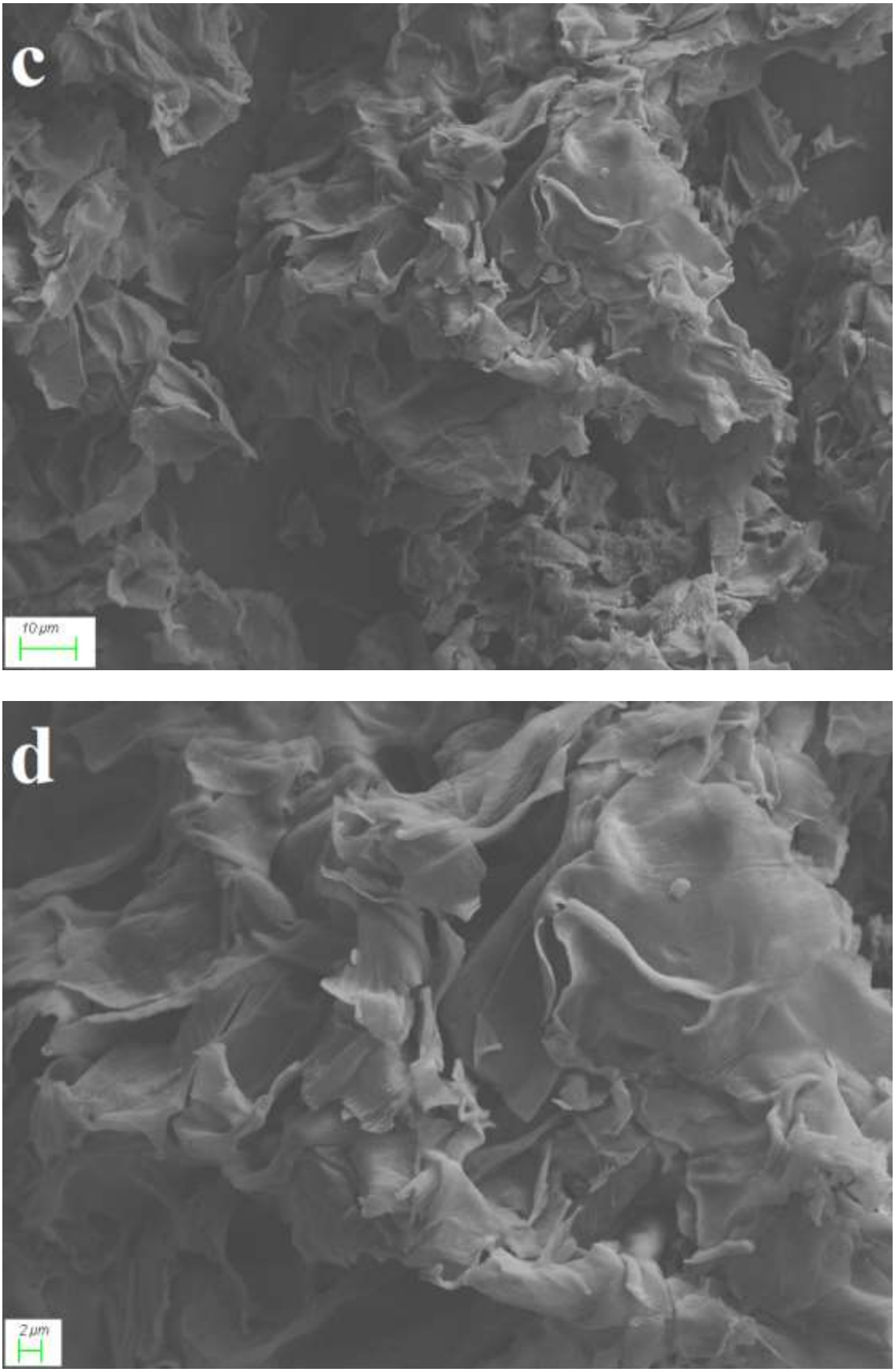

Figure 19. SEM image of AC-4

3.1.5. CO_2 adsorption

Figure 20 depicts the adsorption isotherms of carbon dioxide on the produced activated carbons, as well as the commercial sample.

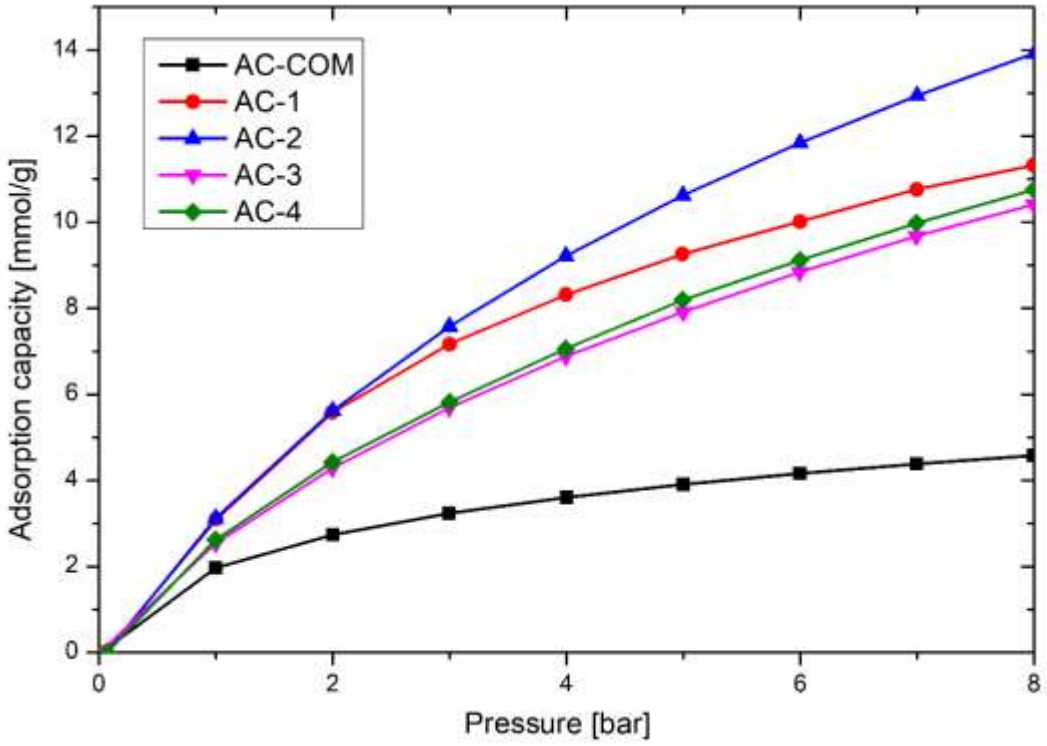

Figure 20. CO_2 adsorption isotherms on AC samples

At the first glance, the superiority of the produced biomass based ACs, over commercially coal based sample, is noticeable. At the atmospheric pressure, the difference between the adsorption capacity of AC-COM and produced samples was from 5.20 to 62.73%, but by increasing the adsorption pressure this difference rose immensely, to values between 149.80 to 204.09%, which is very favorable for the pressure swing adsorption (PSA).

It is seen that by increasing the equilibrium pressure, CO_2 uptake on the AC samples increased as well, which is credited to the growth in driving force (pressure gradient) [40]. The shape of isotherms for the produced ACs was monotonically concaved and categorized as type I, although less steep than isotherm of other adsorbents such as zeolites, MOFs or even the commercial coal based activated carbon, AC-COM.

This implies that regeneration process is easier at PSA process which means more efficient system.

Interestingly, the isotherms showed an unexpected result. Despite to its lower surface area, the carbon dioxide adsorption capacity of the samples activated by KOH was higher than samples activated with NaOH. The reason for this unexpected result can be found in the pore pattern of the samples. As it is mentioned in Table 9, for 60 min activation, samples activated by NaOH (AC-3) had 6% less micropore to the total volume ratio (V_μ/V_T), than KOH activated samples (AC-1). However, this difference for the samples with 120 min carbonization increased to 10%. Meaning, even though NaOH provided a higher total surface area, it resulted in lower micropore over total volume. Additionally, by the Table 9, the average pore diameter of AC-1 and AC-2 was 0.7 and 0.6 nm smaller than the pore diameter of AC-3 and AC-4, respectively. These all determine the superiority of KOH to produce higher micropore density over NaOH. These unpredicted properties of NaOH activated carbon was reported before, in previous studies [41, 52]

For CO_2 adsorption, the concept of "pore size engineering" has been generally accepted [53, 54]. A large surface area and volume of pores in micropore region preferably with size of 0.5 – 0.7 nm (ultra-microporous) are required for high CO_2 selectivity. They have higher potential in carbon dioxide adsorption compare to other micropore or mesopore areas [10]. Therefore, because of higher micropore to total volume ratio and smaller average pore diameter, AC-1 and AC-2 which were activated by KOH showed better carbon dioxide adsorption performance than, AC-3 and AC-4 samples which are activated by NaOH. These are the most important outcomes for engineering and production of the most efficient adsorbent for carbon capture and storage purposes.

Longer carbonization time was beneficial for the cases of having higher specific surface area values, higher micropore to total volume ratio and smaller average pore diameter. It also led to higher adsorption capacity at high pressures, as well. Although, at lower pressures, 0 to 3 bars, this advantage is negligible. For working pressure of 0 – 2 bars, the adsorption capacity of the samples with different carbonization time was negligible. For KOH activated samples the measured difference was as 5.75% at 3 bars and increased to 22.98% at 8 bars. This difference was much lower for NaOH activated samples. At 3 bars, 120 min carbonization only gave 2.44% higher adsorption capacity than 60 min process, and this difference hardly rose to 3.32% at 8 bars.

A comparison of CO_2 adsorption capacity on various modified biomass based activated carbons and samples produced at this study, at the pressure of 8 bars and room temperature (25 °C), is illustrated in Table 10. By this comparison, it is seen that AC-2 has relatively high capacity among the others. From the samples studied for this comparison, only the eucalyptus based AC, modified by ammonia at 800 °C has a higher CO_2 uptake (14.06 mmol/g) than AC-2. AC-4 also exhibits an acceptable CO_2 adsorption performance (10.87 mmol/g) between the other discussed samples. High capacity of the eucalyptus based ACs can be related to the structure of the biomass precursor or the performed activation and modification methods. For a better and more accurate comparison it is suggested to use same activation procedures on both sunflower pith and eucalyptus wood. Nonetheless, selection of the biomass precursor is highly dependent on the agricultural condition and products of each region, where ACs are produced at.

Table 10. Comparison of adsorption capacity of the synthesized AC samples at 8 bars and 25 °C.

Adsorbent	CO_2 Uptake [mmol/g]	Refs.
Eucalyptus wood – H_3PO_4 – Unmodified	10.12	[36]
Eucalyptus wood – H_3PO_4 – Ammonia 400	3.96	[36]
Eucalyptus wood – H_3PO_4 – Ammonia 800	14.06	[36]
Arundo donax – 0:1 KOH	3.00	[37]
Arundo donax – 1:1 KOH	5.93	[37]
Arundo donax – 2:1 KOH	7.12	[37]
Arundo donax – 3:1 KOH	11.17	[37]
Coconut shell based - CSAC	7.72	[40]
AC-COM	4.58	This work
AC-2	13.92	This work
AC-4	10.87	This work

The adsorption capacity of AC-2, the highest adsorption uptake among the produced ACs, was measured at different temperatures to investigate the impact of temperature on the CO_2 uptake, Figure 21. As expected, by increasing the adsorption temperature, the carbon dioxide adsorption capacity of the tested sample decreased,

which was an indication for exothermic nature of the CO_2 adsorption on activated carbon. With the rising the adsorption temperature, the bindings that attached adsorbent and adsorbate together weaken and therefore the adsorption capacity decreases [5]. This case was predicted by the Langmuir equation of adsorption isotherms, which was discussed in chapter 1.

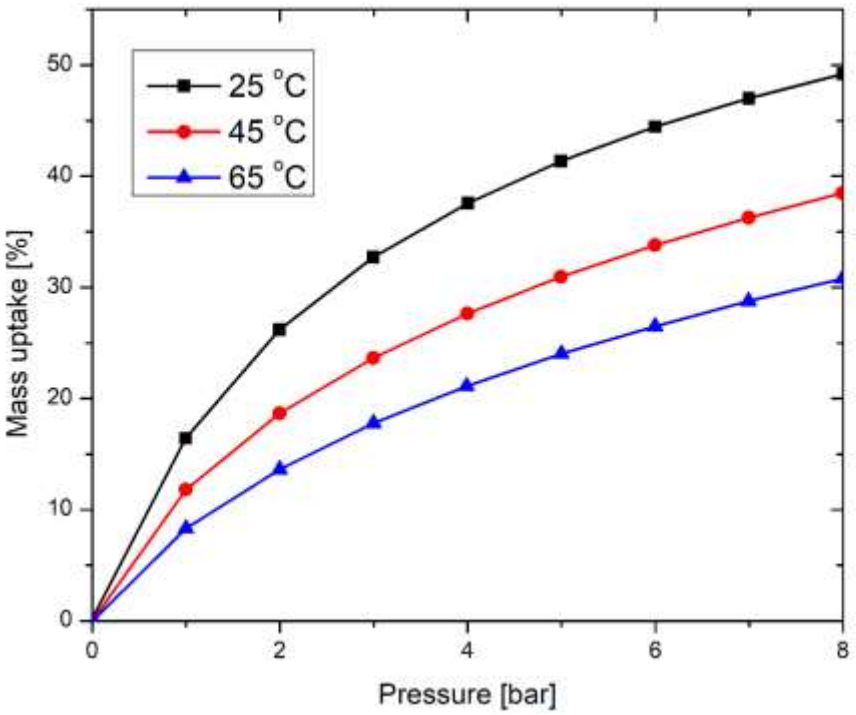

Figure 21. CO_2 adsorption isotherms on AC-2 at different temperatures

3.1.6. Isosteric heat of adsorption

The strength of bonding between adsorbed carbon dioxide molecules and the adsorbent can be determined by measuring the isosteric heat of adsorption (ΔH_{ads}) [37]. This calculation is an important aspect of the design and the development of a carbonaceous adsorbent. To quantify this value, the Langmuir adsorption equation is needed [55]:

$$\theta = \frac{m}{m_\infty} = \frac{KP}{1 + KP}$$

where θ, P and K are equilibrium surface coverage, pressure and the adsorption-desorption ratio, respectively. Besides, m and m_∞ represent the adsorbed mass and the

required mass to complete a monolayer adsorption. To calculate the monolayer mass, m_∞, the following relation can be used [56]:

$$\frac{P}{m} = \frac{P}{m_\infty} + \frac{1}{Km_\infty}$$

Therefore, the plot of the adsorbed CO_2 mass, P/m, versus the adsorption pressure, P, would be linear and its slope represents the inverse of the monolayer mass, Figure 22.

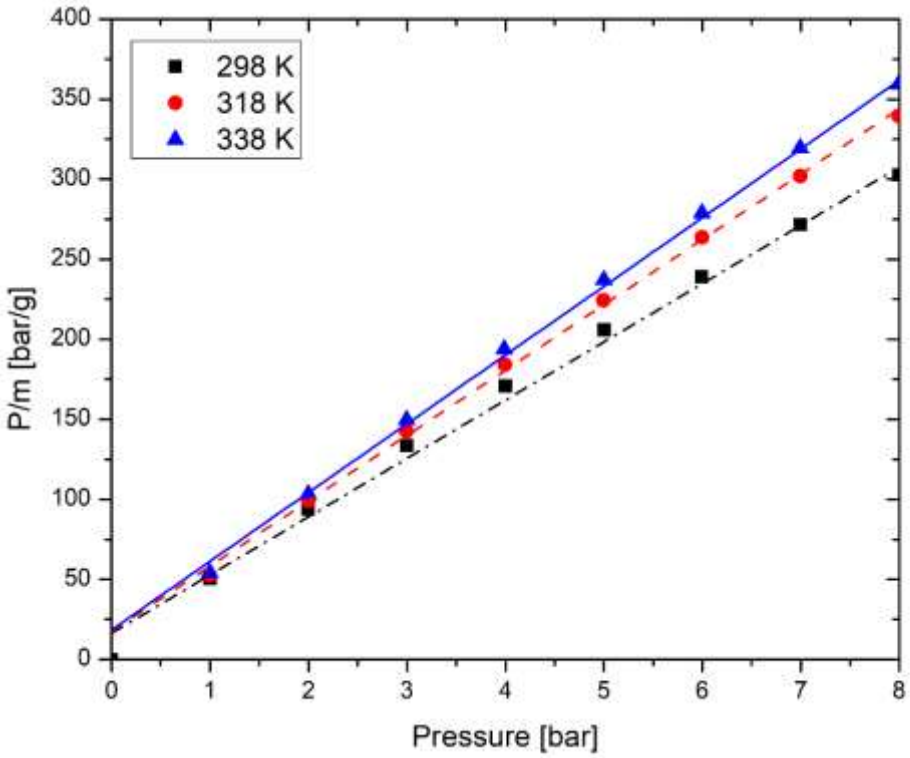

Figure 22. Plot of *P/m* versus *P* for different adsorption temperatures.

The calculated values of m_∞ at 298, 318 and 338 K were 27.47, 24.50 and 23.31 mg, respectively. By having the monolayer and adsorbed CO_2 mass, the Langmuir isotherms of the surface coverage in respect to the adsorption pressure were plotted, which are illustrated in Figure 23.

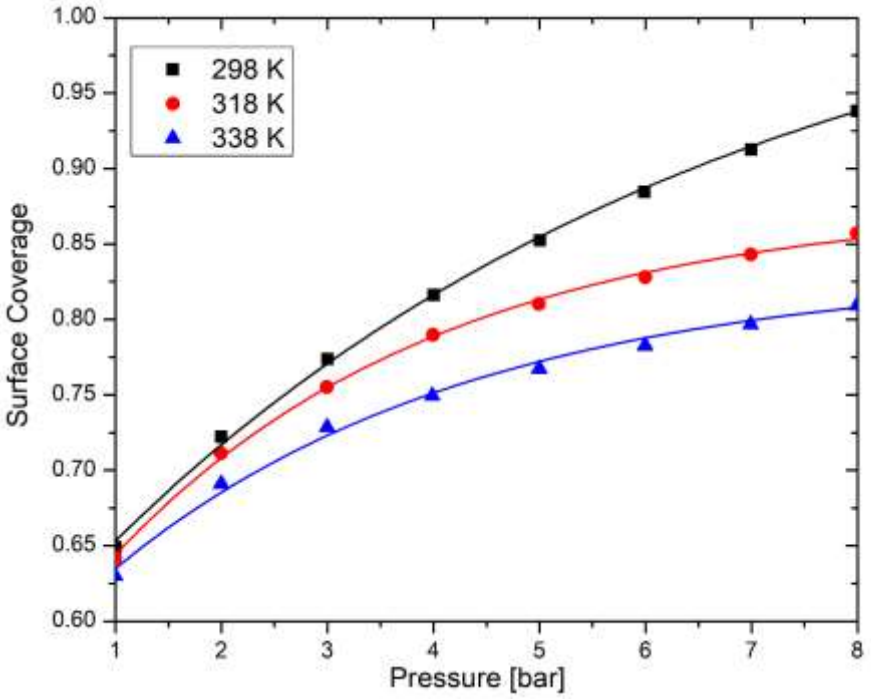

Figure 23. Langmuir adsorption isotherm (surface coverage versus pressure)

At this point, by taking logarithms and derivative with respect to temperature, at a constant surface coverage, the Langmuir equation turns to:

$$\left(\frac{\partial \ln P}{\partial T}\right)_{\theta} = -\left(\frac{\partial \ln K}{\partial T}\right)_{\theta}$$

As discussed in the first chapter, the adsorption and desorption constant ratio, *K*, can be expressed as

$$K = K_0 e^{-\left({}^{\Delta H_{ads}}/_{RT}\right)}$$

where K_0 and R are the adsorption equilibrium pre-exponential factor and the gas constant, respectively. T in this equation represents the adsorption temperature. By merging the equations together, at a constant surface coverage the Langmuir's equation becomes

$$\left(\frac{\partial \ln P}{\partial \left({}^{1}/_{T}\right)}\right)_{\theta} = \frac{\Delta H_{ads}}{R}$$

Therefore, a plot of *ln P* against *1/T* should be a straight line of slope $\Delta H_{ads}/R$. By the plot sketched for the sample AC-2, Figure 24, the isosteric heat of adsorption can be determined as $\Delta H_{ads} = -13.88, -8.73$ and -6.55 kJ/mol for 0.80, 0.75 and 0.70

surface coverage, respectively. These values are typical for CO_2 adsorption on activated carbon. Parshetti et al. calculate the heat range from -23.26 to -18.69 kJ/mol for their EFB biomass based AC samples [57]. Also, ΔH_{ads} values of -26, -31 and -22 kJ/mol were reported for Arundo donax based samples [37]. The negative values of ΔH_{ads} specified the exothermic nature of CO_2 adsorption. Besides, these values are less than the required energy for covalent bonding of carbon dioxide and activated carbon which indicates that physisorption is the dominant process during CO_2 adsorption on activated carbon [37].

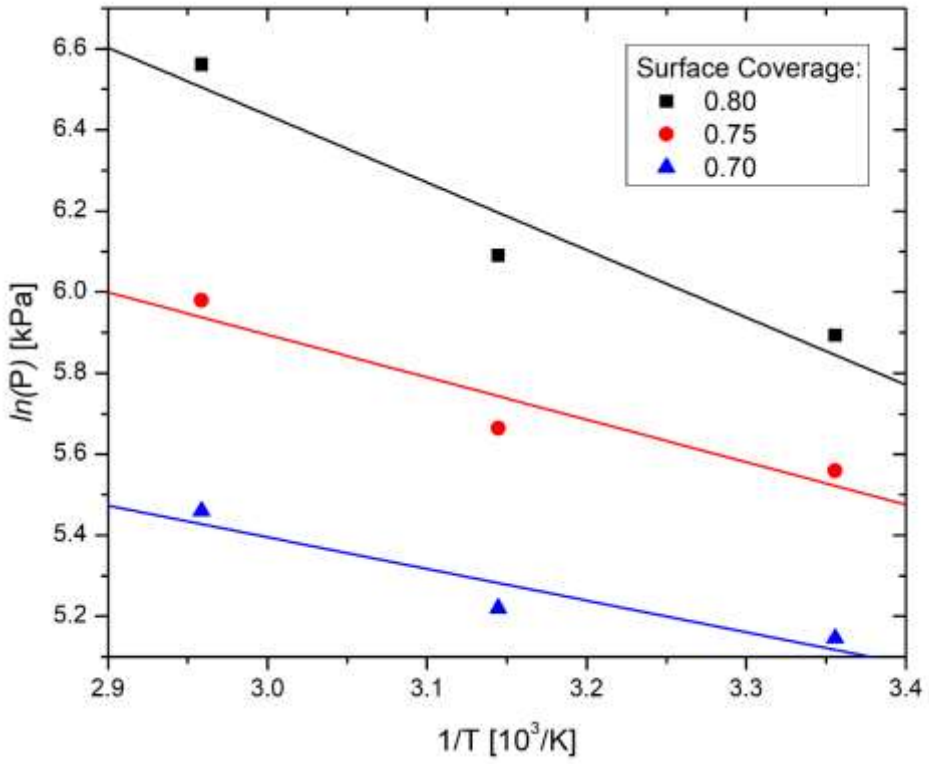

Figure 24. Plot of *ln P* versus *1/T* for various CO_2 uptakes.

3.2. Conclusion

The present study demonstrated the carbon dioxide adsorption on activated carbons produced from sunflower pith, as a local waste agricultural biomass source. Activated carbons are suggested as one of the best candidates for CO_2 adsorption and carbon capture and storage purposes. The superiority of ACs over other adsorbents is because of lower production costs, easier synthesizing, higher adsorption capacity and higher stability in different operating conditions. The AC samples produced from biomass materials, agricultural residues specifically, have shown better carbon dioxide separation and reduced the raw material costs significantly.

The raw biomass material carbonized in a neutral atmosphere provided by nitrogen flow, at different temperatures and duration. It was observed that by increasing the carbonization temperature, more functional groups eliminated from the structure of the raw precursor. The bio-chars produced at 500 °C had the least functional groups remaining in their structures. Increasing the carbonization time, did not make any difference in the functional groups of samples produced at each temperature but reduced the density of them. Longer carbonization time translated to lower functional group density and smoother spectrums.

Furthermore, higher temperature and longer carbonization provided higher BET surface area in the synthesized bio-char samples. The bio-char samples produced at 500 °C with 120 and 60 min carbonization time, with surface area values of 5.35 and 5.11 m^2/g respectively, had 55.52 and 48.54% higher surface area that samples from 350 °C and 30 min carbonization. These two bio-char samples were chosen for the activation process.

The activation step contained both chemical and physical activation. Produced bio-char were mixed with the activation agent and received thermal treatment afterward. Two alkali hydroxides of NaOH and KOH were selection for the role of activation agents. Structural characteristics and adsorption capacity of the synthesized activated carbons were compared with a commercially available coal-based AC sample.

Total surface area of 2948.43 and 2267.52 m^2/g was measured for ACs activated by NaOH and KOH from samples with 120 min carbonization, respectively. These values were 291.1 and 200.77% higher than of the commercial sample. The cellulose structure

of sunflower pith as the precursor and using alkali hydroxides as activation agent translated to a higher surface area over the traditional coal-based AC. By extending the carbonization time from 60 to 120 min, BET surface area of the ACs increased by 10.93 and 7.5% for NaOH and KOH activated samples, respectively. By the pore density analysis of the produced samples and their N_2 adsorption isotherms, it was determined that the biomass based ACs consist of microporous regions. The micropore to total volume ratio for NaOH and KOH activated samples were measured as 68 and 78%, which indicated the advantage of KOH to activated higher micropores despite the lower provided surface area than NaOH. This ratio for the commercial sample was measured as 34% which described it more of a mesoporous material than microporous.

To investigate the carbon dioxide separation performance of the synthesized samples, a CO_2 adsorption test was conducted on them at the pressure range of 0 – 8 bars. The adsorption capacity of the samples increased by increasing the pressure, as expected from the adsorption isotherms. The maximum capacity of the samples as was calculated as 13.92 and 10.75 millimoles of CO_2 per each gram of AC, for KOH and NaOH activated samples. Higher adsorption capacity provided by KOH cannot be explained by surface area results but with pore size distribution of samples. For CO_2 smaller pore diameter in the microporous area is more favorable and leads to higher CO_2 selectivity rather than wider micropores or even mesopores. KOH as the activation agent provided a higher ratio of micropore to total volume and also smaller average pore diameter, therefore a higher CO_2 adsorption capacity was achieved. It should be considered that the adsorption of this study was between 0 to 8 bars. It is possible for NaOH activated samples to exceed adsorption capacity of KOH activated samples at higher pressures. Adsorption test for higher pressures is required to understand the performance of produced adsorbents for a wider range of working pressures. Also, studying adsorption models, such as Langmuir or Dubinin-Astakhov, would be quite helpful to understand the nature of CO_2 adsorption on synthesized AC samples.

Duration time for carbonization did not make any significant difference in carbon separation for samples activated by NaOH. At most 3% more adsorption was achieved by increasing carbonization time from 60 to 120 min. In the case of KOH activated ACs, this rate became more significant; 22.98% at 8 bars. But for lower pressures of 0 to 2 bars samples with different carbonization time, exhibited same adsorption performance. Therefore, in the case of using NaOH activated AC for a CO_2 adsorption system, it is

beneficial to carbonize biomass precursor for 60 minutes instead of 120 minutes. The same situation is recommended for an operation pressure range of 0 to 3 bars on KOH activated samples. By halving the carbonization duration, a considerable amount of energy and time would be saved, which is a vital parameter for engineering of an efficient system.

By the thermodynamic analysis of AC-2, the sample which held the highest CO_2 adsorption capacity, provided valuable information for better understanding of the adsorption mechanism. The value of the isosteric heat of adsorption, ΔH_{ads}, was calculated as -13.88, -8.73 and -6.55 kJ/mol at 298, 318 and 338 K, from the isotherm data for the samples. Decreasing the enthalpy of adsorption and its magnitude, indicated that capturing CO_2 on activated carbon is naturally an exothermic and physisorption process.

The advantage of the synthesized biomass based activated carbon over commercial coal based sample was apparent in every tests and results. Moreover, using a local waste biomass was another advantage of this study, which reduces initial costs. At each location abundant biomass wastes can be used as an effective precursor to produce activated carbon and apply them in CO_2 separation or other objectives. Extra investigations are required to select the best activation process and activation agents. Even different biomass materials can give different characteristics such as surface area or micropore volume.

In the end, production of an effective activated carbon for CO_2 adsorption from biomass waste material was a successful result of this study, but more important than that, it was concluded that to develop an adsorbent for carbon dioxide separation there are three important elements:

1. Chemical structure
2. Surface area
3. Pore size distribution

Each element should be considered in a different level. By engineering and controlling each parameter it would be possible to produce the perfect CO_2 adsorbent and develop the best CCS system.

“It’s time to come together. What’s important is not what’s gone, but what remains. We know that the solutions are there, today. We all have the power to change.

So, what are we waiting for?”

− Home, 2011

REFERENCES

[1] IEA, *CO2 Emissions from Fuel Combustion 2017*, 2017 ed., 2017.

[2] O. Tarasova, A. Vermeulen, and M. Ueno, "The state of greenhouse gases in the atmosphere using global observations through 2015," in *EGU General Assembly Conference Abstracts*, 2017, p. 8824.

[3] A. Samanta, A. Zhao, G. K. Shimizu, P. Sarkar, and R. Gupta, "Post-combustion CO2 capture using solid sorbents: a review," *Industrial & Engineering Chemistry Research*, vol. 51, pp. 1438-1463, 2011.

[4] M. Jalali and F. Aboulghazi, "Sunflower stalk, an agricultural waste, as an adsorbent for the removal of lead and cadmium from aqueous solutions," *Journal of Material Cycles and Waste Management*, vol. 15, pp. 548-555, 2013.

[5] V. K. Singh and E. A. Kumar, "Measurement and analysis of adsorption isotherms of CO 2 on activated carbon," *Applied Thermal Engineering*, vol. 97, pp. 77-86, 2016.

[6] D. Aaron and C. Tsouris, "Separation of CO2 from flue gas: a review," *Separation Science and Technology*, vol. 40, pp. 321-348, 2005.

[7] M. E. Boot-Handford, J. C. Abanades, E. J. Anthony, M. J. Blunt, S. Brandani, N. Mac Dowell, *et al.*, "Carbon capture and storage update," *Energy & Environmental Science*, vol. 7, pp. 130-189, 2014.

[8] J. Wilcox, *Carbon capture*: Springer Science & Business Media, 2012.

[9] M. M. Hossain and H. I. de Lasa, "Chemical-looping combustion (CLC) for inherent CO2 separations—a review," *Chemical Engineering Science*, vol. 63, pp. 4433-4451, 2008.

[10] M. Oschatz and M. Antonietti, "A search for selectivity to enable CO 2 capture with porous adsorbents," *Energy & Environmental Science*, vol. 11, pp. 57-70, 2018.

[11] C.-H. Yu, C.-H. Huang, and C.-S. Tan, "A review of CO2 capture by absorption and adsorption," *Aerosol Air Qual. Res*, vol. 12, pp. 745-769, 2012.

[12] K. Sing, D. Everett, R. Haul, L. Moscou, R. Pierotti, J. Rouquerol, *et al.*, "Physical and biophysical chemistry division commission on colloid and surface chemistry including catalysis," *Pure Appl. Chem*, vol. 57, pp. 603-619, 1985.

[13] M. Thommes, K. Kaneko, A. V. Neimark, J. P. Olivier, F. Rodriguez-Reinoso, J. Rouquerol, *et al.*, "Physisorption of gases, with special reference to the evaluation

of surface area and pore size distribution (IUPAC Technical Report)," *Pure and Applied Chemistry,* vol. 87, pp. 1051-1069, 2015.

[14] S. A. Rackley, *Carbon capture and storage*: Butterworth-Heinemann, 2017.

[15] M. Gray, K. Champagne, D. Fauth, J. Baltrus, and H. Pennline, "Performance of immobilized tertiary amine solid sorbents for the capture of carbon dioxide," *International Journal of Greenhouse Gas Control,* vol. 2, pp. 3-8, 2008.

[16] D. Adams, *Flue gas treatment for CO2 capture*: IEA Clean Coal Centre London, 2010.

[17] A. W. Chester and E. G. Derouane, *Zeolite characterization and catalysis*: Springer, 2009.

[18] S. Coriani, A. Halkier, A. Rizzo, and K. Ruud, "On the molecular electric quadrupole moment and the electric-field-gradient-induced birefringence of CO2 and CS2," *Chemical Physics Letters,* vol. 326, pp. 269-276, 2000.

[19] R. V. Siriwardane, M.-S. Shen, and E. P. Fisher, "Adsorption of CO2, N2, and O2 on natural zeolites," *Energy & fuels,* vol. 17, pp. 571-576, 2003.

[20] R. H. Huesca, J. P. Arcos, D. V. Hernández, and M. A. P. Cruz, "ADSORPTION KINETICS OF N2O ON NATURAL ZEOLITES," *Revista Internacional de Contaminación Ambiental,* vol. 32, pp. 237-242, 2016.

[21] N. T. Nguyen, H. Furukawa, F. Gándara, H. T. Nguyen, K. E. Cordova, and O. M. Yaghi, "Selective Capture of Carbon Dioxide under Humid Conditions by Hydrophobic Chabazite-Type Zeolitic Imidazolate Frameworks," *Angewandte Chemie,* vol. 126, pp. 10821-10824, 2014.

[22] H. Furukawa, K. E. Cordova, M. O'Keeffe, and O. M. Yaghi, "The chemistry and applications of metal-organic frameworks," *Science,* vol. 341, p. 1230444, 2013.

[23] S.-Y. Lee and S.-J. Park, "A review on solid adsorbents for carbon dioxide capture," *Journal of Industrial and Engineering Chemistry,* vol. 23, pp. 1-11, 2015.

[24] A. Cadiau, K. Adil, P. Bhatt, Y. Belmabkhout, and M. Eddaoudi, "A metal-organic framework–based splitter for separating propylene from propane," *Science,* vol. 353, pp. 137-140, 2016.

[25] V. K. Singh and E. A. Kumar, "Experimental investigation and thermodynamic analysis of CO 2 adsorption on activated carbons for cooling system," *Journal of CO2 Utilization,* vol. 17, pp. 290-304, 2017.

[26] D. M. Ruthven, *Encyclopedia of separation technology*: Wiley, 1997.

[27] H. Al-Swaidan and A. Ahmad, "Synthesis and characterization of activated carbon from Saudi Arabian dates tree's fronds wastes," in *Proceedings of the 3rd International Conference on Chemical, Biological and Environmental Engineering, vol. 20*, 2011, pp. 25-31.

[28] T. Tay, S. Ucar, and S. Karagöz, "Preparation and characterization of activated carbon from waste biomass," *Journal of Hazardous Materials,* vol. 165, pp. 481-485, 2009.

[29] E. Köseoğlu and C. Akmil-Başar, "Preparation, structural evaluation and adsorptive properties of activated carbon from agricultural waste biomass," *Advanced Powder Technology,* vol. 26, pp. 811-818, 2015.

[30] R. Saxena, V. K. Singh, and E. A. Kumar, "Carbon dioxide capture and sequestration by adsorption on activated carbon," *Energy Procedia,* vol. 54, pp. 320-329, 2014.

[31] B. Guo, L. Chang, and K. Xie, "Adsorption of carbon dioxide on activated carbon," *Journal of Natural Gas Chemistry,* vol. 15, pp. 223-229, 2006.

[32] P. T. Williams and A. R. Reed, "Development of activated carbon pore structure via physical and chemical activation of biomass fibre waste," *Biomass and Bioenergy,* vol. 30, pp. 144-152, 2006.

[33] M. C. Ribas, M. A. Adebayo, L. D. Prola, E. C. Lima, R. Cataluña, L. A. Feris, *et al.*, "Comparison of a homemade cocoa shell activated carbon with commercial activated carbon for the removal of reactive violet 5 dye from aqueous solutions," *Chemical Engineering Journal,* vol. 248, pp. 315-326, 2014.

[34] A. C. Martins, O. Pezoti, A. L. Cazetta, K. C. Bedin, D. A. Yamazaki, G. F. Bandoch, *et al.*, "Removal of tetracycline by NaOH-activated carbon produced from macadamia nut shells: kinetic and equilibrium studies," *Chemical Engineering Journal,* vol. 260, pp. 291-299, 2015.

[35] A. L. Cazetta, A. M. Vargas, E. M. Nogami, M. H. Kunita, M. R. Guilherme, A. C. Martins, *et al.*, "NaOH-activated carbon of high surface area produced from coconut shell: kinetics and equilibrium studies from the methylene blue adsorption," *Chemical Engineering Journal,* vol. 174, pp. 117-125, 2011.

[36] A. Heidari, H. Younesi, A. Rashidi, and A. A. Ghoreyshi, "Evaluation of CO2 adsorption with eucalyptus wood based activated carbon modified by ammonia solution through heat treatment," *Chemical Engineering Journal,* vol. 254, pp. 503-513, 2014.

[37] G. Singh, I. Y. Kim, K. S. Lakhi, P. Srivastava, R. Naidu, and A. Vinu, "Single step synthesis of activated bio-carbons with a high surface area and their excellent CO2 adsorption capacity," *Carbon,* vol. 116, pp. 448-455, 2017.

[38] A. González, M. Plaza, F. Rubiera, and C. Pevida, "Sustainable biomass-based carbon adsorbents for post-combustion CO2 capture," *Chemical engineering journal,* vol. 230, pp. 456-465, 2013.

[39] T. Song, J.-m. Liao, J. Xiao, and L.-h. Shen, "Effect of micropore and mesopore structure on CO2 adsorption by activated carbons from biomass," *New Carbon Materials,* vol. 30, pp. 156-166, 2015.

[40] V. K. Singh and E. A. Kumar, "Thermodynamic analysis of single-stage and single-effect two-stage adsorption cooling cycles using indigenous coconut shell based activated carbon-CO2 pair," *International Journal of Refrigeration,* vol. 84, pp. 238-252, 2017.

[41] F.-C. Wu and R.-L. Tseng, "High adsorption capacity NaOH-activated carbon for dye removal from aqueous solution," *Journal of hazardous materials,* vol. 152, pp. 1256-1267, 2008.

[42] M. Lillo-Ródenas, D. Cazorla-Amorós, and A. Linares-Solano, "Understanding chemical reactions between carbons and NaOH and KOH: an insight into the chemical activation mechanism," *Carbon,* vol. 41, pp. 267-275, 2003.

[43] H. Zhao, Z. Lai, and A. Firoozabadi, "Sorption Hysteresis of Light Hydrocarbons and Carbon Dioxide in Shale and Kerogen," *Scientific reports,* vol. 7, p. 16209, 2017.

[44] D. Özçimen and A. Ersoy-Meriçboyu, "Characterization of biochar and bio-oil samples obtained from carbonization of various biomass materials," *Renewable Energy,* vol. 35, pp. 1319-1324, 2010.

[45] A. Basta, V. Fierro, H. El-Saied, and A. Celzard, "2-Steps KOH activation of rice straw: an efficient method for preparing high-performance activated carbons," *Bioresource technology,* vol. 100, pp. 3941-3947, 2009.

[46] K. Qian, A. Kumar, K. Patil, D. Bellmer, D. Wang, W. Yuan, *et al.*, "Effects of biomass feedstocks and gasification conditions on the physiochemical properties of char," *Energies,* vol. 6, pp. 3972-3986, 2013.

[47] P. Adapa, C. Karunakaran, L. Tabil, and G. Schoenau, "Qualitative and quantitative analysis of lignocellulosic biomass using infrared spectroscopy," in *CSBE/SCGAB Annual Conference: Rodd's Brudenell River Resort; The*

Canadian Society for Bioengineering: Prince Edward Island, Canada, 2009, pp. 12-15.

[48] M. Baysal, K. Bilge, B. Yılmaz, M. Papila, and Y. Yürüm, "Preparation of high surface area activated carbon from waste-biomass of sunflower piths: Kinetics and equilibrium studies on the dye removal," *Journal of Environmental Chemical Engineering,* 2018.

[49] S. S. Brum, M. L. Bianchi, V. L. d. Silva, M. Gonçalves, M. C. Guerreiro, and L. C. A. d. Oliveira, "Preparation and characterization of activated carbon produced from coffee waste," *Química Nova,* vol. 31, pp. 1048-1052, 2008.

[50] Y.-C. Chiang, P.-C. Chiang, and C.-P. Huang, "Effects of pore structure and temperature on VOC adsorption on activated carbon," *Carbon,* vol. 39, pp. 523-534, 2001.

[51] K. S. Walton and R. Q. Snurr, "Applicability of the BET method for determining surface areas of microporous metal− organic frameworks," *Journal of the American Chemical Society,* vol. 129, pp. 8552-8556, 2007.

[52] R.-L. Tseng, "Mesopore control of high surface area NaOH-activated carbon," *Journal of colloid and interface science,* vol. 303, pp. 494-502, 2006.

[53] A. Silvestre-Albero, S. Rico-Francés, F. Rodríguez-Reinoso, A. M. Kern, M. Klumpp, B. J. Etzold, *et al.*, "High selectivity of TiC-CDC for CO2/N2 separation," *Carbon,* vol. 59, pp. 221-228, 2013.

[54] M. Oschatz, M. Leistner, W. Nickel, and S. Kaskel, "Advanced structural analysis of nanoporous materials by thermal response measurements," *Langmuir,* vol. 31, pp. 4040-4047, 2015.

[55] P. Atkins and J. De Paula, *Elements of physical chemistry*: Oxford University Press, USA, 2013.

[56] V. Bolis, "Fundamentals in adsorption at the solid-gas interface. Concepts and thermodynamics," in *Calorimetry and thermal methods in catalysis*, ed: Springer, 2013, pp. 3-50.

[57] G. K. Parshetti, S. Chowdhury, and R. Balasubramanian, "Biomass derived low-cost microporous adsorbents for efficient CO2 capture," *Fuel,* vol. 148, pp. 246-254, 2015.